Rapid evolution of an RNA virus to escape recognition by a rice nucleotide-binding and leucine-rich repeat domain immune receptor

Mélia Bonnamy, Agnès Pinel-Galzi, Lucille Gorgues, Véronique Chalvon, Eugénie Hébrard, Sophie Chéron, Trang Hiêu Nguyen, Nils Poulicard, François Sabot, Hélène Pidon, et al.

Rapid evolution of an RNA virus to escape recognition by a rice NLR immune receptor

Mélia Bonnamy[1], Agnès Pinel-Galzi[1], Lucille Gorgues[1], Véronique Chalvon[1], Eugénie Hébrard[1], Sophie Chéron[1], Tràng Hiếu Nguyen[2], Nils Poulicard[1], François Sabot[2], Hélène Pidon[2,3], Antony Champion[2], Stella Césari[1], Thomas Kroj[1*], Laurence Albar[1*]

[1] PHIM Plant Health Institute, Univ Montpellier, IRD, CIRAD, INRAE, Institut Agro, 34980 Montpellier, France
[2] DIADE, Univ. Montpellier, IRD, 34394 Montpellier, France
[3] Institute for Resistance Research and Stress Tolerance, Julius Kühn Institute, 06484 Quedlinburg, Germany

* These authors contributed equally to this work

Corresponding authors:
Thomas Kroj (Tel: +33 4 99 62 48 62; thomas.kroj@inrae.fr), Laurence Albar (Tel: +33 4 67 41 62 30; laurence.albar@ird.fr)

SUMMARY

(1) Viral diseases are a major limitation for crop production and their control is crucial for sustainable food supply.
(2) We investigated by a combination of functional genetics and experimental evolution the resistance of rice to the rice yellow mottle virus which is among the most devastating rice pathogens in Africa and the mechanisms underlying the extremely fast adaptation of the virus to its host.
(3) We found that the *RYMV3* gene that protects rice against the virus codes for a nucleotide-binding and leucine-rich repeat domain protein (NLRs) from the Mla-like clade of NLRs. RYMV3 detects the virus by forming a recognition complex with the viral coat protein (CP). The virus escapes efficiently from detection by mutations in its CP some of which interfere with the formation of the recognition complex.
(4) This study establishes that NLRs confer also in monocotyledonous plants immunity to viruses and reveals an unexpected functional diversity for NLRs of the Mla clade that were only known as fungal disease resistance proteins. In additions, it provides precise insight into the mechanisms by which viruses adapt to plant immunity and gives important knowledge for the development of sustainable resistance against viral diseases of cereals.

Key words: disease resistance, evolution, immune receptor, nucleotide-binding and leucine-rich immune receptor (NLR), resistance breakdown, rice, rice yellow mottle virus, virus

INTRODUCTION

Plant immunity to viruses relies on two main mechanisms: the absence or modification of plant factors required for virus propagation in the host, and the induction of antiviral defences upon recognition of the virus. Resistances of the first type are inherited in a recessive manner. Their importance is illustrated by the prominent role of translation initiation factors in virus resistance, described in more than 20 plant/virus pathosystems (Sanfaçon, 2015). Resistances of the second type typically rely on single dominant genes coding for nucleotide-binding and leucine-rich repeat domain proteins (NLRs). More than 20 *NLRs* conferring virus resistance have been cloned, mainly from Solanaceous and legume crops and the model *Arabidopsis thaliana* (Kourelis & Van der Hoorn, 2018; Kourelis *et al.*, 2021). Small RNA-based mechanisms are also crucial in antiviral defence but none of their elements act as major resistance genes (Yang & Li, 2018).

Rice yellow mottle virus (RYMV) is a major threat to rice production in Sub Saharian Africa where it can cause complete harvest losses in case of seedling infection on susceptible varieties (Kouassi *et al.*, 2005; Traoré *et al.*, 2015; Suvi *et al.*, 2021). RYMV is a single-stranded positive-sense RNA virus of the *Sobemovirus* genus in the *Solemoviridae* family whose genome of 4,450-nucleotides (nt) harbors five overlapping open reading frames (ORFs) (Somera *et al.*, 2021). In-depth analysis of RYMV diversity revealed a strong geographical structure (Pinel-Galzi *et al.*, 2015). Transmission of RYMV is mechanical by plant to plant contacts and wounding during agricultural practices, and can be mediated unspecifically by different insect and animal vectors such as beetles, rats and cows, which renders its control particularly challenging (Traore *et al.*, 2009). Sources of strong resistance to RYMV are extremely rare in Asian rice, *Oryza sativa*, which is the most cultivated rice species, and occur more frequently in African cultivated rice, *Oryza glaberrima* (Thiemele *et al.*, 2010). Three resistance genes, *rymv1*, *rymv2* and *RYMV3*, have been characterized. *rymv1* and *rymv2* are both inherited in a recessive manner and code, respectively, for a eukaryotic translation initiation factor, eIF(iso)4G1 and a putative nucleoporin (Albar *et al.*, 2006; Orjuela *et al.*, 2013; Pidon *et al.*, 2020). *RYMV3* acts in a dominant way and fine mapping in the *O. glaberrima* accession Tog5307 identified the ortholog of the Nipponbare *NLR Os11g43700* as the best candidate gene (Pidon *et al.*, 2017).

NLRs form huge gene families in plant genomes with several hundred to more than a thousand members and confer resistance to pests from various kingdoms such as viruses, fungi, bacteria or nematodes (Kourelis *et al.*, 2021). They act as intracellular receptors that detect viral proteins or pathogen virulence effectors inside host cells and trigger immune responses, frequently comprising a so-called hypersensitive response and programmed cell death. The recognition of the pathogenic proteins that trigger incompatibility and that are therefore called avirulence (Avr) factors, occurs either by direct interaction with the NLR, or indirectly through NLR-mediated detection of their activity on a host protein. This host protein may either be the effector target protein or a decoy protein that mimics the genuine effector target and thus serves as an effector trap (Cesari, 2018; Kourelis & van der Hoorn, 2018). NLRs have a conserved architecture characterized by a C-terminal leucine-rich repeat (LRR) domain that is crucial in effector recognition and a central nucleotide-binding (NB) domain that serves as a molecular switch regulating the activity of the receptor and mediating self-association upon activation (Burdett *et al.*, 2019; Wang & Chai, 2020). At their N-terminus, they carry a variable signaling domain that is most frequently either an interleukin-1 receptor (TIR) domain or a coiled-coil (CC) domain and that divides plant NLRs into the TNL and the CNL subgroups. Some NLRs harbor, in addition, non-canonical integrated domains (IDs) that act presumably as decoy domains in effector recognition and are thought to be derived from true effector targets (Cesari *et al.*, 2014).

In this study, we found that the RYMV3 resistance is conferred by a single *NLR* gene that belongs to a monocot-specific subclade previously known to confer resistance to pathogenic fungi only. We identified the coat protein (CP) of the virus as the Avr factor and show that the CP associates with the RYMV3 immune receptor for recognition. Finally, we demonstrate the virus adapts to RYMV3 resistance through mutations in the CP that abolish its recognition and, in some cases, its association to the NLR receptor.

MATERIALS AND METHODS

Generation of transgenic rice

Agrobacterium tumefaciens (strain EHA101)-mediated transformation was performed on the *O. sativa* Kitaake variety (Sallaud *et al.*, 2003). The NLR_{CDS} construct included the complete CDS of the candidate NLR allele from the resistant Tog5307 *O. glaberrima* accession (Genebank MT348369.1). It was synthesized by GeneCust and cloned between the Ubiquitin promoter and the Nos terminator in the pCAMBIA-5300 binary vector. The NLR_G construct contained a genomic fragment covering 2,2kb upstream of the ATG to 0.7kb downstream of the STOP codon. It was amplified with the Phusion High-Fidelity DNA Polymerase (Thermo Fisher) from the DNA of Tog5307 accession using primers NLR-F2 and NLR-R2 (see primer sequences in Table S1 and construct characteristics in Table S2) and cloned with the Gateway system (Thermofisher) into the pCAMBIA-1300-GW vector that was adapted to insertion of genomic clones by LR reaction. Genotyping of progenies was performed by PCR as described in Orjuela *et al*. (2013). Presence/absence of the transgene was checked based on the amplification of the *hygromycin resistance* gene, with HygR-F and HygR-R primers, and then confirmed with the amplification of *RYMV3*, using primer pairs Ubi/NLR-R1, targeting the NLR_{CDS} construct, or NLR-S10R/NLR-R8, targeting the NLR_G construct, that does not amplify the native copy of the NLR in Kitaake.

Viral material and rice infection assays

Wild type RYMV isolates used in this study originated from Burkina-Faso (BF1), Côte d'Ivoire (CI2, CI3, CI8), Madagascar (Mg1), Mali (Ma10), Niger (Ng106), Togo (Tg274) and Tanzania (Tz2, Tz3, Tz5, Tz9, Tz211) (Table S3). They were multiplied on *O. sativa* ssp. *indica* IR64 variety. Leaf samples of symptomatic Tog5307 plants were obtained from Pidon *et al*. (2017). Mutants CIa*CP:37M, CIa*CP:163D and CIa*CP:230W were constructed by directed mutagenesis of the infectious clone obtained by Brugidou *et al.* (1995) using the CIa isolate from Côte d'Ivoire (Table S3). Mutagenesis was performed with the QuickChange Site-Directed Mutagenesis Kit (Stratagene), as described in Poulicard *et al.* (2012). The coat protein sequences of the set of 595 RYMV isolates described in Issaka *et al*. (2021) was used to analyse the variability of the CP in natural populations. This set of RYMV isolates comprised 261 isolates from West and Central Africa, 240 isolates from East Africa and 94 isolates from Madagascar.

Rice plants were grown in greenhouse conditions with 28°C/26°C day/night temperature. Plants were mechanically inoculated with RYMV using grinded infected leaves about 2 weeks after sowing as described in Pinel-Galzi *et al*. (2018), except for the CIa infectious clone and its variants that were transcribed in vitro with T7 RNA polymerase (Promega) and inoculated *in planta* as described in Brugidou *et al*. (1995). Back-inoculation assays consists in one cycle of re-infection using extracts from leaves collected from symptomatic Tog5307 plants in the study of Pidon et al. (2017). Resistance evaluations were based on symptoms observed between 2 and 4 weeks after inoculation. In some cases, ELISA tests were performed to confirm resistance, as described in Pinel-Galzi *et al.* (2018). The *O. sativa* Kitaake and IR64 varieties were used as susceptibility controls and *O. glaberrima* Tog5307 as resistance one.

Phylogenetic analysis

The sequences of resistance proteins of grasses classified as CNL by Kourelis & van der Hoorn (2018), and the sequence of the N TNL resistance protein from *Nicotiana glutinosa* were retrieved from Genebank (Table S4). NB-ARC (PFAM00931) domains were identified based on Genebank annotations or on a PFAM analysis. RYMV3 homologs in the reference accession of rice, Nipponbare, were identified by blasting the NB-ARC domain of *RYMV3-R* on the protein sequences annotated from MSU RGAP release 7 (Kawahara *et al.*, 2013). The 40 best hits were conserved. Alignments were performed with MAFFT v7.407_1 and then trimmed using BMGE v1.12_1 using NGPhylogeny web service (Lemoine *et al.*, 2019). Phylogenetic trees were constructed using maximum likelihood-based inference with smart selection model (PhyML+SMS 1.8.1-1; Guindon *et al.*, 2010; Lefort *et al.*, 2017), on the ATGC Montpellier Bioinformatics Platform. Branch supports were estimated with SH-like aLTR. Synteny analysis was performed with Genomicus (Nguyen et al., 2018).

RYMV full-genome and CP gene sequencing

Full-length sequencing of the viral genome was performed by Illumina sequencing as described in Pinel-Galzi *et al.* (2016). Briefly, two overlapping fragments of the viral genemone were amplified from each sample and pooled to construct the libraries according to the protocol of Mariac *et al.* (2014). A paired-end sequencing (2 x 150 pb) was performed on an Illumina MiSeq v3. Bioinformatics analysis was conducted with the TOGGLEv0.3 suite (Monat *et al.*, 2015) according to Pinel-Galzi *et al.* (2016). The sequence of the CIa isolate (GenBank AJ608219) was used as reference to generate the control sequence of BF1, CI2 and CI8 WT samples and the sequence of the Ni1 isolate (GenBank AJ608212) for Tg274 and Ng109 WT samples. All datasets (including control datasets) were then mapped on the corresponding control sequence. SNP calling was performed using LoFreq software (Wilm *et al.*, 2012). Only SNPs with a quality over 200 were considered. To make the comparison between samples easier, polymorphisms were located on the sequence of the CIa sample, which could generate a shift of 1 or 2 nucleotides from their original position due to small InDels between isolates.

For some samples, sequencing of the CP gene was performed by Sanger. Retrotranscription was performed with ImProm II Retrotranscripase (Promega) and the primer RYMV-4450. Amplification was performed with GoTaq G2 polymerase (Promega) and primer pairs RYMV-3342/RYMV-4207. Sequencing was subcontracted to GeneWiz.

Transient expression assay in *N. benthamiana*

Constructs of rymv3-S susceptibility allele and CP_{Mg1} mutants were obtained by site-directed mutagenesis with a QuikChange Lightning Site-Directed Mutagenesis kit (Agilent Technologies, Santa Clara, USA), on plasmids pDONR207 containing the sequence of the RYMV3-R resistance allele or wild type CP_{Mg1} respectively (see primers in Table S1 and constructs in Table S2). The CP sequences of isolates Tg274, CI2, CI8 and their variants were obtained from RNA extracted from infected *O. sativa* IR64 plants. RNAs were retrotranscribed to cDNA with M-MLV retrotranscriptase (Promega) and amplified by PCR (Phusion High-Fidelity DNA Polymerase (ThermoFisher, Waltham, USA), with primers 3LA-att-CPF/3LA-att-CP-R. PCR products were then introduced into pDONR207 plasmids by BP recombination (ThermoFisher, Waltham, USA). CP sequences of the different isolates, variants and mutants were transferred from pDONR207 to pBIN19-35S-YFP-GW expression plasmid, and RYMV3-R and rymv3-S to pBIN19-35S-GW-3HA expression plasmid using LR reactions (ThermoFisher, Waltham, USA).

pBIN19 constructs were transformed into *A. tumefaciens* GV3101 strain by electroporation. Agroinfiltration and cell death assays were performed and analyzed as described by Xi *et al.* (2021)

CoIP

Co-immunoprecipitation and immunoblotting experiments were performed as previously described (Ortiz *et al.*, 2017) using magnetic beads coated with anti-GFP antibodies (Chromotek) and high stringency washing (50 mM Tris-HCl Ph 7.5, 150 mM NaCl, 1% IGEPAL CA-630, 0.1% SDS, Deoxycholate 0.5%, PMSF 1mM, Complete protease inhibitor cocktail (Roche) and extraction buffer (washing buffer complemented with 1% Protease inhibitor (Sigma), 10 mM DTT, 0.5% PVPP). Detection of horseradish peroxidase-coupled antibodies in western blot experiments was performed using the Immobilon Western Kit (Millipore) or SuperSignal West Femto Maximum Sensitivity Substrate (Thermo Fisher Scientific).

Accession numbers

The genomic and CDS sequences of *Rymv3-R* are registered under accessions numbers ON131778 and MT348369, respectively. The sequence of *rymv3-S* CDS corresponds to the gene model ORGLA11G0175800.1 established on the CG14 accession (Wang et al, 2014). Accessions numbers of NLR genes used for phylogenetic analysis are listed in Table S4. Illumina sequences generated on RYMV variants and corresponding wild-type were deposited in the European Nucleotide Archive (Project PRJEB48932, Sample accessions: SAMEA11293793-SAMEA11293802).

RESULTS

RYMV3 resistance is conferred by a single *NLR*.

The ortholog of the *O. sativa NLR Os11g43700* was previously identified as the best candidate for *RYMV3* in the *O. glaberrima* accession Tog5307 (Pidon *et al.*, 2017). To test whether it confers indeed resistance to RYMV, we introduced this gene by stable transformation into the susceptible *O. sativa japonica* rice variety Kitaake. Two different constructs derived from Tog5307 sequences were used for transgenesis. The NLR_G construct contains a 7.4 kb genomic fragment of the *NLR* including a 2.2 kb promoter sequence upstream of the start codon and a 0.7 kb terminator sequence downstream of the stop codon. The NLR_{CDS} construct comprises the NLR coding sequence (CDS) driven by the maize *ubiquitin* promoter.

After infection with the RYMV isolate BF1, Kitaake wild-type plants showed chlorosis and mottling of leaves while the three independent transgenic lines obtained with the NLR_G genomic construct showed RYMV resistance (Fig. **1a**, Fig. S1, Table S5). T1 generation plants carrying the NLR_G construct remained symptomless after RYMV infection, while sister lines without the transgene developed disease symptoms. Analysis of T2 families confirmed this result since all but one of the 159 plants carrying the NLR_G transgene were resistant to BF1 (Table S5). Susceptibility of this particular T2 plant putatively resulted from resistance-breaking (RB) events, as previously observed in Pidon *et al.* (2017). On healthy plants, no difference in growth and morphology was observed between transgenic and Kitaake wild-type plants.

For the NLR_{CDS} construct, we obtained only one single informative transgenic line. All other transgenic lines created with this construct were either sterile in the T0 generation or had lost the NLR_{CDS} transgene and carried only the *hygromycin resistance* gene indicating a strong selection against the transgene. In the single transgenic line carrying NLR_{CDS}, the transgene perfectly co-segregated with RYMV resistance in T1 and T2 plants (Fig. **1a**, Fig. S1, Table S5).

Taken together, these complementation experiments confirmed that the candidate *NLR* at the *RYMV3* locus confers RYMV resistance and is thus the *RYMV3* gene. The allele from Tog5307 conferring RYMV resistance is therefore in the following referred to as *RYMV3-R*, while the susceptible allele from *O. glaberrima* accession CG14 (gene *ORGLA11g0175800*) is called *rymv3-S*. Their products differ only by residue 779 located in the LRR domain, which is an arginine (R) in the resistant allele and a lysine (K) in the susceptible variant (Pidon *et al.*, 2017; Pidon *et al.*, 2020).

RYMV3 is closely related to Sr35 and MLA-like NLRs.

For an initial characterization of RYMV3, we compared its sequence to that of 32 CNL resistance proteins from grasses (Table S4). Phylogenetic analysis based on an alignment of the amino acid sequence of the NB-ARC domain, which is the most conserved domain in NLRs, revealed that among rice resistance proteins, RYMV3-R is most closely related to Pi36 that confers resistance to the fungus *Pyricularia oryzae,* the causal agent of blast disease (Fig. S2, Fig. S3) (Liu *et al.*, 2007). In addition, RYMV3-R is closely related to the stem rust resistance protein Sr35 from *Triticum monococcum* (Saintenac *et al.*, 2013) and to the powdery mildew resistance protein MLA from barley and *Triticum monococcum* and its orthologs Sr33 and Sr50 from *Aegilops tauschii* and *Secale cereale* that both confer resistance to stem rust (Seeholzer *et al.*, 2010; Periyannan *et al.*, 2013; Mago *et al.*, 2015) (Fig. **1b**, Fig. S2, Fig. S3, Fig. S4, Table S6). This similarity with MLA and MLA-like NLRs was confirmed in an analysis that included, in addition, the 40 closest homologs of RYMV3-R in the *Oryza sativa* reference cv. Nipponbare (Fig. S5, Fig. S6). However, *RYMV3* and *Mla* are in different regions of the genome. The loci containing *Mla* and its orthologs are synthenic to a region on chromosome 5 of rice (Periyannan *et al.*, 2013) while the *RYMV3* locus that is located on rice chromosome 11 is syntenic to a region of the chromosomes 4A, 4B and 4D of *T. aestivum*, and 4H of *H. vulgare*.

Escape from *RYMV3* resistance correlates with mutations in the viral CP.

We previously observed sporadic infection events with multiple incompatible RYMV isolates on the resistant *O. glaberrima* accession Tog5307, which is the donor of *RYMV3-R* (Pidon *et al.*, 2017). To investigate whether these infections resulted from resistance-breakdown or incomplete penetrance of resistance, we performed back-inoculation assays with extracts from leaves collected from symptomatic Tog5307 plants in the study of Pidon *et al.* (2017). Twenty symptomatic Tog5307 leaf samples collected after inoculation with the wild-type isolates BF1, CI8, CI2, CI3, Ng106, Tg274, Ng109 or Mg1 were used as inoculum sources to

re-infect Tog5307 and the susceptible *O. sativa* control IR64. All samples were infectious on IR64, although, in some instances, infectivity appeared to be lower than that of the corresponding wild-type isolate (Fisher test, p<0,05; Fig. **2a**, Table S7). Fifteen samples were more infectious on Tog5307 than their respective wild-type controls, indicating evolution of the virus towards escape from RYMV3 resistance in Tog5307 (Fisher test, p<0,05; Fig. **2a**, Table S7). For five samples, no significant differences with the wild-type isolates were observed, which may reflect rare cases of incomplete resistance in the initial assay (i.e. in the case of the CI2 V1, Ng109 V1, V2 and V3 samples) or low fitness of the evolved variants in the samples used for re-inoculation (i.e. Mg1 V1 sample).

Eight samples used in the back-inoculation tests (BF1 V1 and V2, CI8 V1, CI2 V1 and V2, Tg274 V1 and V2, Ng109 V1) were selected for full RYMV genome sequencing using Illumina technology. Corresponding RYMV wild-type samples collected on the susceptible variety IR64 were sequenced as references (Table S8). Alternate variants with a frequency above 0.05 in at least one sample were detected at 53 sites (Table S9). In wild-type samples, the frequency of alternate variants was generally low and never exceeded 0.24. A particularly high number of polymorphic sites were detected, and confirmed in two independent replicates of the CI8 wild-type, which suggests that this sample is a mix of two genotypes. Among the samples collected on Tog5307, 15 polymorphic sites were identified with an alternate variant frequency above 0.05 in at least one sample (Table S9). The alternate variant frequencies were below 0.44 for 5 sites and above 0.98 in the remaining 10 indicating that these alternate variants had been strongly selected. The polymorphic sites were distributed all over the genome with a clustering of sites characterized by non-synonymous and highly selected variants in the region coding for the coat protein (CP) (Fig. **2b**). Interestingly, these polymorphic sites in the CP were not detected in the wild-type samples, while most of the polymorphisms outside the CP were also detected with low frequencies (f<0,05) in the corresponding wild-type samples, suggesting that these variants were pre-existing in the inoculum. Six of the seven non-synonymous polymorphic sites in the CP were almost fixed for the alternate variant (i.e. Q39R, S41P, A93V, G163D, R166Q, and R230W, which was found in 3 different isolates) and all eight samples collected on Tog5307 carried at least one of those mutations (Fig. **2b**).

To deepen this analysis, we sequenced the *CP* of 14 additional samples from symptomatic Tog5307 plants using Sanger sequencing. Nine of them (BF1 V3, CI8 V2 and V3, CI3 V1 and V2, Ng106 V1 and V2, Tg274 V3, Mg1 V1) had been analyzed in the back-inoculation tests previously described (Fig. **2a**). The five others (Ni1 V1, V2 and V3 ; Tz211 V1 and V2) had not because no significant increase of infection rate was expected du to the high infection rate already observed with the Ni1 and Tz211 WT isolates (Pidon *et al.*, 2017). Non-synonymous mutations in the CP were detected in all the samples, except the two deriving from Tz211, which further supports the crucial role of the CP in RYMV3 resistance (Fig. **2c**). In total, targeted *CP*-sequencing identified 6 new mutations (P36R, P36S, V37M, W56S, R103W and I224N) and 6 cases with the previously identified mutations A93V, G163D or R230W (Fig. **2c**). These three mutations that were detected multiple times and in different isolates are therefore of particular interest. Interestingly the Tz211 wild-type and derived samples collected on Tog5307 carried at position 37 a methionine instead of a valine, which was also found in the RB variant Ni1-V2. This could explain the high infectivity of the Tz211 wild type isolate and its capacity to infect Tog5307 without the acquisition of any new mutation.

To further extend this analysis and monitor the variability of the CP in natural populations, we analyzed the CP sequence diversity in a panel of 595 RYMV isolates that is representative of the diversity of the virus and described in Issaka *et al.* (2021). This showed that the CP residues that are mutated in the RB variants are highly conserved in natural populations (Table 1). Residues P36, Q39, S41, W56, A93, D130, G163, R166, I224 and R230 were conserved in all or all but one or two isolates and only positions 37 and 103 were variable, with, respectively, 25 and 14 isolates with alternate residues. Except for position 37, in no case, the residue identified in RB variants was observed in field isolates (Table 1**,** Fig. **2c**). On the contrary, all 14 isolates with alternate residues at position 37 had the methionine, previously described in a RB variant of Ni1 and in the Tz211 wild-type isolate. Thirteen CP_M37 isolates, including Tz211, are from Tanzania and one, Ma10, is from Mali. Inoculation experiments with four additional M37 isolates (Ma10, Tz2, Tz3 and Tz9) showed that these isolates are highly infectious on Tog5307 (Table S10). These results indicate that CP polymorphisms in natural RYMV populations allow escape from RYMV3 resistance but that the frequency of such RB variants is low, probably due to the absence of selection for this character.

To confirm the role of CP mutations in escape from RYMV3 resistance, we introduced the V37M, G163D and R230W substitutions in the CIa infectious clone (Brugidou *et al.*, 1995) by directed mutagenesis providing mutants CIa*CP:V37M, CIa*CP:G163D and CIa*CP:R230W. After *in vitro* transcription, the mutant RNAs were inoculated on ten Tog5307 and ten IR64 plants. For CIa*CP:G163D and CIa*CP:R230W transcripts, no infection on Tog5307 and only four infected IR64 plants were observed two weeks post-inoculation (Table S11). We confirmed by Sanger sequencing that the mutations of the *CP* were conserved in infected plants. Two IR64 infected samples for each mutant were then used for a back-inoculation test on the same accessions. No or only few (not more than 20%) infection events were observed on both IR64 and Tog5307 suggesting that these *CP* mutations strongly attenuate the viral fitness of the infectious clone. With the CIa*CP:V37M transcript, all inoculated IR64 and Tog5307 plants were infected confirming that this mutation breaks RYMV3 resistance without a strong impact on virus fitness (Table S11).

Taken together, these data indicate that RYMV adapts to resistance in Tog5307 by selecting specific mutations in the CP and that this enables escape from RYMV3-mediated recognition. This suggests that the NLR RYMV3 recognizes the CP.

RYMV3 recognizes the CP of RYMV.

To test the hypothesis that the CP is recognized by RYMV3 and to analyze how the K/R polymorphism in the LRR domain that distinguishes rymv3-S and RYMV3-R affects this recognition, we performed cell death assays in *Nicotiana benthamiana*. We first tested whether both RYMV3 alleles trigger, like other MLA-like NLRs, autonomous cell death in this system. For this, we performed *Agrobacterium tumefaciens*-mediated expression of the complete CDS of the resistant (*RYMV3-R*) and susceptible (*rymv3-S*) alleles of *RYMV3* under the control of the *35S* promoter and with, or without, a C-terminally fused HA tag. All constructs except *rymv3-S:HA* triggered cell-death, which demonstrates autoactivity of both RYMV3-R and rymv3-S in *N. benthamiana* (Fig. **3**). However, the lysine (K) at position 779 in rymv3-S or the addition of a C-terminal HA tag to RYMV3-R strongly reduced autoactivity. Indeed, for RYMV3-R, strong confluent cell-death was already induced with an *Agrobacterium* concentration of OD_{600}=0.05, while a five times higher inoculum (OD_{600}=0.25) was required for *rymv3-S* and *RYMV3-R:HA (*Fig. **3**). The complete loss of autoactivity with *rymv3-S:HA* may be a consequence of the combination of these two effects. However, this does not involve destabilization of the protein since rymv3-S:HA and RYMV3-R:HA were detected at equal levels in immunoblotting experiments (Fig. S7a).

To test whether RYMV3-R recognizes the RYMV CP, we co-expressed both proteins in *N. benthamiana* cell death assays. The *RYMV3-R:HA* and *rymv3-S* constructs, which have the same level of autoactivity, were infiltrated at an inoculum density of OD_{600}=0.05 at which they do not trigger cell-death (Fig. **3**, Fig. S8). The CP of the isolate Mg1 was fused to YFP and a construct with YFP alone was used as a control. The proper expression of the different proteins, except rymv3-S, was confirmed by immunoblotting (Fig. S7a). The co-expression of YFP:CP_{Mg1} with RYMV3-R:HA triggered strong cell-death (Fig. **4**). This confirmed the recognition of the CP by RYMV3-R. In contrast, no cell-death was observed upon co-expression of YFP:CP_{Mg1} and rymv3-S, suggesting that the K779 residue is sufficient to abolish the recognition of the CP by RYMV3.

CP mutations associated with resistance breakdown abolish recognition by RYMV3-R.

To test if the RB mutations in the CP directly interfere with its detection by RYMV3-R, the CP of the isolates Tg274, CI2 and CI8, and of four of their RB variants were expressed together with RYMV3-R in *N. benthamiana*. The selected variants included mutations A93V, G163D and R230W, which were identified multiple times and therefore appear to be particularly suited for resistance breakdown. The co-expression of RYMV3-R:HA with the wild type CP constructs YFP:CP_{Tg274}, YFP:CP_{CI2} or YFP:CP_{CI8} induced the same level of cell-death as YFP:CP_{Mg1} (Fig. **5)**. With the mutant constructs YFP:CP_{CI2}-G163D, YFP:CP_{Tg274}-R230W, YFP:CP_{Tg274}-A93V and YFP:CP_{CI8}-R230W, the cell-death response was drastically reduced and not significantly different from the YFP control. Immunoblotting showed that the mutant CPs were expressed at similar levels as the corresponding wild-type CPs (Fig. S7b,c,d). These results indicate that these CP mutations enable RB by preventing recognition of the CP by RYMV3-R in plant cells.

To further verify this hypothesis and to compare the effect of these mutations in a common background, we introduced the A93V, G163D and R230W substitutions in the CP of the Mg1 isolate, for which no RB variant carrying these mutations had been re-isolated (Fig. **2a,c**). YFP:CP_{Mg1}-A93V did not induce a cell death response upon co-expression with RYMV3-R:HA, while the response was strongly reduced with YFP:CP_{Mg1}-G163D and YFP:CP_{Mg1}-R230W (Fig. **5a,e**). Immuno-blotting showed that the mutant and wild-type CP_{Mg1} were expressed at similar levels (Fig. S7e). These results confirm that RYMV3 resistance relies on detection of the CP by RYMV3 and indicate that the modification of specific single residues of the CP enables the virus to escape perception and immunity.

CP recognition involves the formation of RYMV3-CP complexes.

To investigate whether detection of the CP by RYMV-R involves the association of both proteins in a recognition complex, we performed co-immunoprecipitation (co-IP) experiments. RYMV-R:HA and rymv3-S:HA were co-expressed with YFP:CP_{Mg1} in *N. benthamiana* and anti-GFP immunoprecipitation was performed. YFP alone and the rice CNL RGA4-HA that confers together with the CNL RGA5 resistance to the fungus *P. oryzae* served as negative controls (Cesari *et al.*, 2013; Cesari *et al.*, 2014). Analysis of input samples by immunoblotting with anti-HA and anti-GFP antibodies confirmed that all proteins were correctly expressed (Fig. **6**). The immunoprecipitation of YFP:CP_{Mg1} with anti-GFP antibodies co-precipitated RYMV3-R:HA but not rymv3-S nor the RGA4 control. This result indicates that RYMV3-R specifically associates with the CP and that this complex is allele-specific as rymv3-S does not.

The co-IP experiments were repeated with the CP_{Mg1} mutant variants A93V, G163D and R230W to analyze whether RB mutations in the CP act by interfering with the formation of RYMV3/CP complexes. The efficient co-immunoprecipitation of RYMV3-R by CP_{Mg1} was strongly reduced by the A93V and G163D mutations but not by the R230W mutation (Fig. **6**). This suggests that A93V and G163D interfere with the formation of RYMV3-R/CP complexes which may cause the escape from the NLR immune receptor-mediated recognition, while the R230W mutation does not affect the strength of the association of CP with RYMV3-R and therefore seem to act by another mechanism.

DISCUSSION

RYMV3 resistance relies on formation of a protein complex between a CNL immune receptor and the CP.

In this study, we found that the *R* gene *RYMV3* from African rice *O. glaberrima* is an *NLR* through genetic complementation of a susceptible *O. sativa* variety. Functional studies in the heterologous *N. benthamiana* model system further validate the gene identity. While *NLR*s are the largest class of disease resistance genes and confer immunity to all types of pathogenic organisms, they had not yet been described to confer resistance to viruses in monocotyledonous plants, and in particular not in cereals (Kourelis *et al.*, 2021). Dominant resistance to viruses is frequent in cereals. The corresponding genes have been in many cases genetically characterized and *NLR*s have been frequently identified as candidate genes suggesting that, also in cereals, they are a major class among dominant virus *R* genes (Wu *et al.*, 2007; Zhao *et al.*, 2010; Lu *et al.*, 2011; Okada *et al.*, 2020; Pidon *et al.*, 2021). Our study lends strong support to this hypothesis and suggests that monocot immunity to viruses also largely relies on the intracellular recognition of viral proteins by NLRs.

We also identify the CP of the virus as the Avr factor recognized by RYMV3. We show that sporadic infections on the *O. glaberrima RYMV3* donor accession Tog5307 result from RB events, and that all RB variants carry non-synonymous mutations in the genomic sequence coding for the CP. This indicates an extremely rapid adaptation of the virus in experimental conditions by selection of non-synonymous mutations in one single gene. Amino acid changes at 12 different positions were identified all over the CP sequence and several of them multiple times. One of them, V37M, was also found in field isolates where it is also associated with escape from RYMV3 resistance. Introduction of the V37M mutation into the infectious RYMV clone CIa conferred virulence on Tog5307. These results compellingly identify the CP as the Avr factor detected by RYMV3. We further validated this hypothesis in the heterologous *N. benthamiana* system

where the CP was detected by RYMV3 in an allele-specific manner since expression of the CP with RYMV3-R but not with rymv3-S triggered cell death. In addition, introduction of RB mutations into the CP abolished or strongly attenuated recognition in this heterologous system.

Among the 16 known viral Avr factors detected by plant NLRs, 8 are CPs which makes them the largest class of viral proteins recognized by these immune receptors (Sekine *et al.*, 2012; de Ronde *et al.*, 2014; Kim *et al.*, 2015; Kim *et al.*, 2017; Grech-Baran *et al.*, 2020; Shen *et al.*, 2020). Possible reasons for the preference of NLRs for CP recognition are their high abundance from the beginning of the infection on and at all stages, their multi-functionality and their central role throughout the infection process in all different classes of plant viruses. The CP_{RYMV}/RYMV3 system appears therefore as a very representative and canonical Avr/NLR system in plant virus immunity.

Using co-IP experiments, we established that detection of the CP involves the formation of a recognition complex comprising the CP and RYMV3-R. rymv3-S that differs in only one single residue in the LRR domain (K at position 779 instead of R) does not form this complex. Whether this association involves direct binding between the partner proteins could not be established since Y2H experiments did not detect physical interaction between RYMV3 and the CP. CP recognition may therefore rely on an additional co-factor bound by both proteins and, potentially, conserved between rice and *N. benthamiana*.

Analysis of RB mutations in co-IP experiments revealed that two of them, A93V and G163D, drastically reduce complex formation. This links the evolutionary mechanism of RYMV3 RB that consists in the evolution of the CP for escape from recognition by RYMV3 with the molecular mechanism of CP detection that relies on the association of the CP with RYMV3 and that is strongly attenuated by RB mutations.

RYMV3 is an MLA-like CNL

Phylogenetic analysis classed *RYMV3* into the *Mla*-like subclade of Poaceae specific CNLs. This subclade contains numerous resistance genes against pathogenic fungi and has been thoroughly investigated as a model for the diversity and molecular mechanisms of plant NLRs. Most studied and diversified are the *Mla* powdery mildew resistance genes from *Mildew locus A* of barley (*Hordeum vulgare*), a complex *CNL* gene cluster. The locus is characterized by high allelic richness and extraordinary structure and sequence variation (Wei *et al.*, 2002; Maekawa *et al.*, 2019). In cultivated barley, 28 allelic *Mla* resistance gene variants have been identified, each conferring specific resistance to different races of *Blumeria graminis* forma specialis (f.sp.) *hordei* (Seeholzer *et al.*, 2010), and, some of them, additionally to the completely unrelated wheat stripe rust fungus *Pucciania striiformis* f. sp *tritici* (Bettgenhaeuser *et al.*, 2021). The *Mla* locus is conserved in the *Triticeae* subtribe where it also shows high diversity. Some of these *Mla* orthologues also act as powdery mildew or rust *R* genes such as *TmMla* from *Triticum monococcum* or *Sr33* and *Sr50* from, respectively, *Aegilops tauchii* and rye (*Secale cereale*) (Jordan *et al.*, 2011; Periyannan *et al.*, 2013; Mago *et al.*, 2015). Additional resistance genes that belong to the same *CNL* subclade are *Sr35*, from *T. monococcum* and *Pi36* from rice that confers resistance against the fungus *Pyricularia oryzae* (Liu *et al.*, 2007; Saintenac *et al.*, 2013). Identification of *RYMV3* demonstrates that the MLA-like subclade of CNLs is a hotspot of disease resistance diversity in cereals with a much broader functional diversity than the previously documented recognition of fungal pathogens and potentially also harbors members that recognize other types of pathogens than viruses and fungi.

RYMV3 is not clustered with other CNLs in the genome of *O. glaberrima* and *O. sativa*, the locus shows much less structural diversity within and between rice species than the *Mla* locus in Triticeae and the two loci are not in synthenic regions of the genome. Nevertheless, RYMV3 possesses important sequence diversity with at least 11 different haplotypes in *O. glaberrima* differentiated by 34 non-synonymous SNPs, and 112 non synonymous variable sites in *O. sativa* (Pidon et al., 2020). However, it is not known if some of these additional RYMV3 alleles also confer specific recognition of RYMV or other pathogens.

RYMV3 does not only share sequence similarity but also functional features with the characterized CNLs of the MLA-like subclade. Like Sr35, MLAs and their orthologues, RYMV3 triggers cell death in *N. benthamiana* (Bai *et al.*, 2012; Cesari *et al.*, 2016; Bolus *et al.*, 2020). This constitutive immune activation

seems not restricted to the heterologous system as only one transgenic rice plant overexpressing *RYMV3* under control of the strong maize *ubiquitin* promoter could be obtained. All other transgenic plants with this construct either aborted, were sterile in the T0 generation or lost the *RYMV3* transgene, suggesting activation of autoimmunity upon overexpression of RYMV3. In comparison, the NLR_G construct with the endogenous promoter caused no deleterious effects indicating that proper regulation of *RYMV3* is important for cellular integrity.

An additional shared feature among MLA-like CNLs is that the recognition of the avirulence factor can be recapitulated in *N. benthamiana*. Indeed, co-expression of RYMV3 with its corresponding Avr-factor triggers cell death in *N. benthamiana*, as observed when Sr35, Sr50 or multiple MLA alleles are co-expressed with the fungal Avr-factors they recognize (Chen *et al.*, 2017; Salcedo *et al.*, 2017; Saur *et al.*, 2019). In addition, in all cases, recognition involves the formation of a protein complex between the NLR and the recognized pathogen factor. In the cases of Sr50/AvrSr50, Sr35/AvrSr35 and 4 different MLA/AVR_a pairs, complex formation involves direct physical binding which therefore appears as a common feature of many MLA-like CNLs (Chen *et al.*, 2017; Salcedo *et al.*, 2017; Saur *et al.*, 2019; Ortiz *et al.*, 2022). Deeper elucidation of the molecular mechanisms of CP recognition by RYMV3 will therefore provide important insight into the functional diversification between closely related NLRs.

RYMV adaptation to *RYMV3* and resistance durability

The extraordinarily fast adaptation of RYMV to *RYMV3* resistance illustrates the speed and efficiency with which pathogens can adapt to the extreme selection pressure exerted by receptor-mediated immunity in plants. The general mechanism of escape from *RYMV3*-mediated resistance is similar to the one most frequently observed in other pathogenic organisms in response to NLRs. Instead of developing mechanisms to cope with the plant immune response, the virus responds by selecting mutations in the viral component detected by the immune receptor. The high speed with which RYMV can evolve is largely due to the high mutation rate in RNA viruses that results from the lack of proofreading activity of their RNA dependent RNA polymerase responsible for viral replication and their fast and efficient replication that classes them among the fastest evolving organisms on earth (Drake & Holland, 1999). Consequently, similarly rapid adaptation has previously been documented for escape of RYMV from the recessive *rymv1* or *rymv2* resistances by mutations in, respectively, the the viral-protein genome linked (VPg) and the membrane anchor domain of the polyprotein P2a (Hébrard *et al.*, 2006; Traoré *et al.*, 2010; Pinel-Galzi *et al.*, 2016). Interestingly, a similar speed and mechanism of resistance escape was also found in the adaptation of the pepino mosaic virus to *Rx*-mediated resistance in transgenic tomato (Candresse et al., 2010). An escape frequency of 10% was found to be linked to mutations in the viral CP that abolish HR induction in transient *N. benthamiana* assays.

The high number of CP mutations that can lead to escape from recognition by RYMV3 (12 different RB mutations distributed over the entire protein) contrasts with *rymv1* and *rymv2* RB that target only a few specific positions. Substitutions in the VPg are dominated by changes at three positions (Pinel-Galzi *et al.*, 2007; Traoré *et al.*, 2010; Hébrard *et al.*, 2018), and substitutions in the polyprotein P2a mainly occur at one single site (Pinel-Galzi *et al.*, 2016). This may reflect that in recessive resistances RB is caused by a gain of function and that only a limited number of sites can restore function. Indeed, the specific polymorphisms in the resistance *rymv1* alleles of rice eIF(iso)4G1 abolish the interaction with the VPg and RB mutations counteract the effect of the polymorphisms and restore this interaction (Hébrard *et al.*, 2010). On the contrary, escape from RYMV3 resistance can be considered as a loss of function, i.e. loss of formation of a functional recognition complex that triggers immunity. It can be assumed that such a loss of function can be achieved more easily than gain of functions, even if CP evolution is constrained by its original functions that must not be affected to avoid strong fitness penalties.

The fast RB of RYMV3 under experimental conditions does not necessarily indicate low durability under field conditions. In fact, it is hardly possible to extrapolate to the field level from experimental evolution focused exclusively on the intra-host scale since RB integrates successive trade-offs at intra-host, inter-host and environmental levels (Moreno-Perez *et al.*, 2016). The small genome size of viruses, with overlapping ORFs and multifunctional proteins, increases the constraint to virus evolution, compared to cellular pathogens, which may explain why resistances to viruses are often more durable than resistance to cellular

pathogens (Fraile & Garcia-Arenal, 2010). RB mutations have to pass successfully different stringent selection steps before emerging at the field level and may still be associated with strong fitness costs. The failure to validate some RB mutations by directed mutagenesis and the low infection rate of certain evolved variants on both susceptible and resistant genotypes probably reflects a high fitness cost of these mutations in particular viral genetic backgrounds. However, the V37M mutation present in one RB variant was also present in the natural diversity of the virus, where it was also associated with the ability to infect Tog5307. This mutation emerged twice, in different RYMV lineages: once in East Africa in isolates of the S5 strain and once in Wes-t Africa in the Ma10 isolate from the S1 strain. This mutation was retained although varieties carrying *RYMV3-R* are scarcely cultivated, suggesting that this mutation does not strongly impair the infectivity of the virus on susceptible varieties. The V37M polymorphism appears therefore as a major threat to *RYMV3-R* durability.

Taken together, our study establishes a unique example for the detection of a virus by an MLA-like CNL immune receptor in cereals and provides a compelling example for the efficient adaptation of a pathogen to the extreme selection pressure exerted by a plant immune receptor. It reveals the molecular mechanisms underlying the adaptation of RYMV to a plant immune receptor and it provides important insight into the durability potential of this resistance.

Aknowledgements

This work was supported by the CGIAR Research Program on rice agri-food systems (RICE, 2017–2022) and the Investissements d'Avenir Program (Labex Agro: ANR-10-LABX-001-01) . We thank C. Dubreuil-Tranchant for her help in bioinformatics analysis and the IRD itrop Plant and Health bioinformatic platform for providing HPC resources and support for our research project. We thank M. Fournel, H. Chrestin and M. Rous for technical help. We thank S. Lacombe for the CP-Mg1 construct. We thank, Diana Ortiz, Naranayia Upadhyaya and Isabelle Saur for yeast two hybrid constructs.

Author contributions

T.K. and L.A. designed the research. M.B., A.P.G., L.G., V.C., E.H., S.Ch., T.H.N., N.P., H.P., A.C., S.Ce., L.A. performed the experiments. M.B., E.H., N.P., F.S., S.Ce., T.K., L.A. analyzed the data. M.B., T.K., L.A., S.Ce wrote the article. T.K. and L.A. contributed equally to this work. All authors read and commented on the article.

Data availability

The data that supports the findings of this study are available in the supplementary material of this article or are available from the corresponding author upon reasonable request.

References

Albar L, Bangratz-Reyser M, Hébrard E, Ndjiondjop M-N, Jones M, Ghesquière A, Hebrard E, Ndjiondjop M-N, Jones M, Ghesquière A. **2006**. Mutations in the eIF(iso)4G translation initiation factor confer high resistance of rice to Rice yellow mottle virus. *Plant Journal* **47**: 417–426.

Bai S, Liu J, Chang C, Zhang L, Maekawa T, Wang Q, Xiao W, Liu Y, Chai J, Takken FLW, *et al.* 2012. Structure-function analysis of barley NLR immune receptor MLA10 reveals its cell compartment specific activity in cell death and disease resistance. *PLOS Pathogens* **8**: e1002752.

Bettgenhaeuser J, Hernandez-Pinzon I, Dawson A, Gardiner M, Green P, Taylor J, Smoker M, Ferguson J, Emmrich P, Hubbard A, *et al.* 2021. The barley immune receptor Mla recognizes multiple pathogens and contributes to host range dynamics. *Nature Communications* **12**: 6915.

Bolus S, Akhunov E, Coaker G, Dubcovsky J. **2020**. Dissection of cell death induction by wheat stem rust resistance protein Sr35 and its matching effector AvrSr35. *Molecular Plant-Microbe Interactions* **33**: 308–319.

Brugidou C, Holt C, Yassi M N, Zhang S, Beachy RN, Fauquet C. **1995**. Synthesis of an infectious full-length cDNA clone of rice yellow mottle virus and mutagenesis of the coat protein. *Virology* **206**: 108–115.

Burdett H, Kobe B, Anderson PA. **2019**. Animal NLRs continue to inform plant NLR structure and function. *Archives of Biochemistry and Biophysics* **670**: 58–68.

Candresse T, Marais A, Faure C, Dubrana MP, Gombert J, Bendahmane A. 2010. Multiple Coat Protein Mutations Abolish Recognition of Pepino mosaic potexvirus (PepMV) by the Potato Rx Resistance Gene in

Transgenic Tomatoes. *Molecular Plant-Microbe Interactions* **23**: 376–383.

Cesari S. **2018**. Multiple strategies for pathogen perception by plant immune receptors. *New Phytologist* **219**: 17–24.

Cesari S, Kansaki H, Fujiwara T, Bernoux M, Chalvon V, Kawano Y, Shimamoto K, Dodds P, Terauchi R, Kroj T. **2014**. The NB-LRR proteins RGA4 and RGA5 interact functionally and physically to confer disease resistance. *The EMBO Journal* **33**: 1941–1959.

Cesari S, Moore J, Chen C, Webb D, Periyannan S, Mago R, Bernoux M, Lagudah ES, Dodds PN. **2016**. Cytosolic activation of cell death and stem rust resistance by cereal MLA-family CC–NLR proteins. *Proceedings of the National Academy of Sciences* **113**: 10204–10209.

Cesari S, Thilliez G, Ribot C, Chalvon V, Michel C, Jauneau A, Rivas S, Alaux L, Kanzaki H, Okuyama Y, *et al.* 2013. The rice resistance protein pair RGA4/RGA5 recognizes the Magnaporthe oryzae effectors AVR-Pia and AVR1-CO39 by direct binding. *The Plant Cell* **25**: 1463–1481.

Chen J, Upadhyaya NM, Ortiz D, Sperschneider J, Li F, Bouton C, Breen S, Dong C, Xu B, Zhang X, *et al.* 2017. Loss of AvrSr50 by somatic exchange in stem rust leads to virulence for Sr50 resistance in wheat. *Science* **358**: 1607–1610.

Drake JW, Holland JJ. **1999**. Mutation rates among RNA viruses. *Proceedings of the National Academy of Sciences* **96**: 13910–13913.

Fargette D, Pinel A, Abubakar Z, Traore O, Brugidou C, Fatogoma S, Hebrard E, Choisy M, Sere Y, Fauquet C, *et al.* 2004. Inferring the evolutionary history of Rice yellow mottle virus from genomic, phylogenetic, and phylogeographic studies. *Journal of Virology* **78**: 3252–3261.

Fargette D, Pinel A, Rakotomalala M, Sangu E, Traore O, Sereme D, Sorho F, Issaka S, Hebrard E, Sere Y, *et al.* 2008. Rice yellow mottle virus, an RNA plant virus, evolves as rapidly as most RNA animal viruses. *Journal of Virology* **82**: 3584–3589.

Fraile A, García-Arenal F. **2010**. The coevolution of plants and viruses: resistance and pathogenicity. *Advances in Virus Research* **76**: 1–32.

Grech-Baran M, Witek K, Szajko K, Witek AI, Morgiewicz K, Wasilewicz-Flis I, Jakuczun H, Marczewski W, Jones JDG, Hennig J. **2020**. Extreme resistance to Potato virus Y in potato carrying the Rysto gene is mediated by a TIR-NLR immune receptor. *Plant Biotechnology Journal* **18**: 655–667.

Guindon S, Dufayard J-F, Lefort V, Anisimova M, Hordijk W, Gascuel O. **2010**. New algorithms and methods to estimate maximum-likelihood phylogenies: assessing the performance of PhyML 3.0. *Systematic Biology* **59**: 307–321.

Hébrard E, Pinel-Galzi A, Bersoult A, Siré C, Fargette D. **2006**. Emergence of a resistance-breaking isolate of Rice yellow mottle virus during serial inoculations is due to a single substitution in the genome-linked viral protein VPg. *Journal of General Virology* **87**: 1369–1373.

Hébrard E, Pinel-Galzi AA, Oludare A, Poulicard N, Aribi J, Fabre S, Issaka S, Mariac CC, Dereeper A, Albar L, *et al.* 2018. Identification of a hypervirulent pathotype of Rice yellow mottle virus : a threat to genetic resistance deployment in West-Central Africa. *Phytopathology* **108**: 299–307.

Issaka S, Traoré O, Longué RDS, Pinel-Galzi A, Gill MS, Dellicour S, Bastide P, Guindon S, Hébrard E, Dugué M-J, *et al.* 2021. Rivers and landscape ecology of a plant virus, Rice yellow mottle virus along the Niger Valley. *Virus Evolution* **7**: 1–14.

Jordan T, Seeholzer S, Schwizer S, Toller A, Somssich I, Keller B. **2011**. The wheat Mla homologue TmMla1 exhibits an evolutionarily conserved function against powdery mildew in both wheat and barley. *Plant Journal* **65**: 610–621.

Kawahara Y, de la Bastide M, Hamilton JP, Kanamori H, McCombie WR, Ouyang S, Schwartz DC, Tanaka T, Wu J, Zhou S, *et al.* 2013. Improvement of the *Oryza sativa* Nipponbare reference genome using next generation sequence and optical map data. *Rice* **6**: 4.

Kim S-B, Kang W-H, Huy HN, Yeom S-I, An J-T, Kim S, Kang M-Y, Kim HJ, Jo YD, Ha Y, *et al.* 2017. Divergent evolution of multiple virus-resistance genes from a progenitor in Capsicum spp. *New Phytologist* **213**: 886–899.

Kim S-B, Lee H-Y, Seo S, Lee JH, Choi D. **2015**. RNA-Dependent RNA polymerase (NIb) of the Potyviruses is an avirulence factor for the broad-spectrum resistance gene Pvr4 in Capsicum annuum cv. CM334. *PLOS ONE* **10**: e0119639.

Kouassi NKK, N'Guessan P, Albar L, Fauquet CM, Brugidou C. **2005**. Distribution and characterization

of rice yellow mottle virus : A threat to African farmers. *Plant Disease* **89**: 124–133.

Kourelis J, van der Hoorn RAL. **2018**. Defended to the nines: 25 years of resistance gene cloning identifies nine mechanisms for R protein function. *The Plant Cell* **30**: tpc.00579.2017.

Kourelis J, Sakai T, Adachi H, Kamoun S. **2021**. RefPlantNLR is a comprehensive collection of experimentally validated plant disease resistance proteins from the NLR family. *PLOS Biology* **19**: e3001124.

Lefort V, Longueville J-E, Gascuel O. **2017**. SMS: Smart Model Selection in PhyML. *Molecular Biology and Evolution* **34**: 2422–2424.

Lemoine F, Correia D, Lefort V, Doppelt-Azeroual O, Mareuil F, Cohen-Boulakia S, Gascuel O. **2019**. NGPhylogeny.fr: new generation phylogenetic services for non-specialists. *Nucleic Acids Research* **47**: W260–W265.

Liu X, Lin F, Wang L, Pan Q. **2007**. The in Silico map-based cloning of Pi36, a rice coiled-coil-nucleotide-binding site-leucine-rich repeat gene that confers race-specific resistance to the blast fungus. *Genetics* **176**: 2541–2549.

Lu H, Price J, Devkota R, Rush C, Rudd J. **2011**. A dominant gene for resistance to Wheat streak mosaic virus in winter wheat line CO960293-2. *Crop Science* **51**: 5–12.

Maekawa T, Kracher B, Saur IML, Yoshikawa-Maekawa M, Kellner R, Pankin A, Von Korff M, Schulze-Lefert P. **2019**. Subfamily-specific specialization of RGH1/MLA immune receptors in wild barley. *Molecular Plant-Microbe Interactions* **32**: 107–119.

Mago R, Zhang P, Vautrin S, Šimková H, Bansal U, Luo M-C, Rouse M, Karaoglu H, Periyannan S, Kolmer J, *et al.* 2015. The wheat Sr50 gene reveals rich diversity at a cereal disease resistance locus. *Nature Plants* **1**: 1–3.

Mariac C, Scarcelli N, Pouzadou J, Barnaud A, Billot C, Faye A, Kougbeadjo A, Maillol V, Martin G, Sabot F, *et al.* 2014. Cost-effective enrichment hybridization capture of chloroplast genomes at deep multiplexing levels for population genetics and phylogeography studies. *Molecular Ecology Resources*: 1103–1113.

Monat C, Tranchant-Dubreuil C, Kougbeadjo A, Farcy CC, Ortega-Abboud E, Amanzougarene S, Ravel SS, Agbessi MM, Orjuela-Bouniol J, Summo M, *et al.* 2015. TOGGLE: toolbox for generic NGS analyses. *BMC Bioinformatics* **16**: 374.

Moreno-Pérez MG, García-Luque I, Fraile A, García-Arenal F. **2016**. Mutations determining resistance-breaking in a plant RNA virus have pleiotropic effects on its fitness that depend on the host environment and on the type, single or mixed, of infection. *Journal of Virology*: JVI.00737-16.

Nguyen NTT, Vincens P, Roest Crollius H, Louis A. **2018**. Genomicus 2018: karyotype evolutionary trees and on-the-fly synteny computing. *Nucleic Acids Research* **46**: D816–D822.

Okada K, Kato T, Oikawa T, Komatsuda T, Namai K. **2020**. A genetic analysis of the resistance in barley to *Soil-borne wheat mosaic virus*. *Breeding Science* **70**: 617–622.

Orjuela J, Thiémélé DEF, Kolade O, Chéron S, Ghesquière A, Albar L. 2013. A recessive resistance to Rice yellow mottle virus is associated with a rice homolog of the CPR5 gene, a regulator of active defense mechanisms. *Molecular plant-microbe interactions : MPMI* **26**: 1455–63.

Ortiz D, Chen J, Outram MA, Saur IML, Upadhyaya NM, Mago R, Ericsson DJ, Cesari S, Chen C, Williams SJ, *et al.* 2022. The stem rust effector protein AvrSr50 escapes Sr50 recognition by a substitution in a single surface-exposed residue. *New Phytologist* **234**: 592–606.

Ortiz D, de Guillen K, Cesari S, Chalvon V, Gracy J, Padilla A, Kroj T. **2017**. Recognition of the Magnaporthe oryzae Effector AVR-Pia by the Decoy Domain of the Rice NLR Immune Receptor RGA5. *PLANT CELL* **29**: 156–168.

Periyannan S, Moore J, Ayliffe MA, Bansal U, Wang X, Huang L, Deal K, Luo M, Kong X, Bariana H, *et al.* 2013. The gene Sr33, an ortholog of barley Mla genes, encodes resistance to wheat stem rust race Ug99. **6147**: 786–788.

Pidon H, Chéron S, Ghesquière A, Albar L. **2020**. Allele mining unlocks the identification of RYMV resistance genes and alleles in African cultivated rice. *BMC PLant Biology* **20**: 222.

Pidon H, Ghesquière A, Chéron S, Issaka S, Hébrard E, Sabot F, Kolade O, Silué D, Albar L. **2017**. Fine mapping of RYMV3: a new resistance gene to Rice yellow mottle virus from Oryza glaberrima. *Theoretical and Applied Genetics* **130**: 807–818.

Pidon H, Wendler N, Habekuβ A, Maasberg A, Ruge-Wehling B, Perovic D, Ordon F, Stein N. **2021**. High-resolution mapping of Rym14Hb, a wild relative resistance gene to barley yellow mosaic disease. *Theoretical and Applied Genetics* **134**: 823–833.

Pinel A, N'Guessan P P, Boussalem M, Fargette D. **2000**. Molecular variability of geographically distinct isolates of Rice yellow mottle virus in Africa. *Archives of Virology* **145**: 1621–1638.

Pinel-Galzi A, Dubreuil-Tranchant C, Hébrard E, Mariac C, Ghesquière A, Albar L. 2016. Mutations in Rice yellow mottle virus polyprotein P2a involved in RYMV2 gene resistance breakdown. *Frontiers in Plant Science* **7**

Pinel-Galzi A, Hébrard E, Traoré O, Silué D, Albar L. **2018**. Protocol for RYMV Inoculation and Resistance Evaluation in Rice Seedlings. *Bio-protocol* **8**: 1–13.

Pinel-Galzi A, Rakotomalala M, Sangu E, Sorho F, Kanyeka Z, Traoré O, Sérémé D, Poulicard N, Rabenantoandro Y, Séré Y, *et al.* 2007. Theme and variations in the evolutionary pathways to virulence of an RNA plant virus species. *PLoS Pathogens* **3**: 1761–1770.

Pinel-Galzi A, Traoré O, Séré Y, Hébrard E, Fargette D. **2015**. The biogeography of viral emergence: rice yellow mottle virus as a case study. *Current Opinion in Virology* **10**: 7–13.

Poulicard N, Pinel-Galzi A, Traoré O, Vignols F, Ghesquière A, Konaté G, Hébrard E, Fargette D. **2012**. Historical contingencies modulate the adaptability of rice yellow mottle virus. *PLoS Pathogens* **8**: e1002482.

de Ronde D, Butterbach P, Kormelink R. **2014**. Dominant resistance against plant viruses. *Frontiers in Plant Science* **5**: 307.

Saintenac C, Zhang W, Salcedo A, Rouse MN, Trick HN, Akhunov E, Dubcovsky J. **2013**. Identification of wheat gene Sr35 that confers resistance to Ug99 stem rust race group. *Science* **341**: 783–786.

Salcedo A, Rutter W, Wang S, Akhunova A, Bolus S, Chao S, Anderson N, Soto MFD, Rouse M, Szabo L, *et al.* 2017. Variation in the AvrSr35 gene determines Sr35 resistance against wheat stem rust race Ug99. *Science* **358**: 1606.

Sallaud C, Meynard D, van Boxtel J, Gay C, Bès M, Brizard JP, Larmande P, Ortega D, Raynal M, Portefaix M, *et al.* 2003. Highly efficient production and characterization of T-DNA plants for rice (Oryza sativa L.) functional genomics. *Theoretical and Applied Genetics* **106**: 1396–1408.

Sanfaçon H. **2015**. Plant translation factors and virus resistance. *Viruses* **7**: 3392–3419.

Saur I, Bauer S, Kracher B, Lu X, Franzeskakis L, Muller M, Sabelleck B, Kummel F, Panstruga R, Maekawa T, *et al.* 2019. Multiple pairs of allelic MLA immune receptor-powdery mildew AVR(A) effectors argue for a direct recognition mechanism. *ELIFE* **8**: e44471.

Seeholzer S, Tsuchimatsu T, Jordan T, Bieri S, Pajonk S, Yang W, Jahoor A, Shimizu KK, Keller B, Schulze-Lefert P. **2010**. Diversity at the Mla Powdery Mildew Resistance Locus from Cultivated Barley Reveals Sites of Positive Selection. *Molecular Plant-Microbe Interactions* **23**: 497–509.

Sekine K-T, Tomita R, Takeuchi S, Atsumi G, Saitoh H, Mizumoto H, Kiba A, Yamaoka N, Nishiguchi M, Hikichi Y, *et al.* 2012. Functional Differentiation in the Leucine-Rich Repeat Domains of Closely Related Plant Virus-Resistance Proteins That Recognize Common Avr Proteins. *Molecular Plant-Microbe Interactions* **25**: 1219–1229.

Shen X, Yan Z, Wang X, Wang Y, Arens M, Du Y, Visser RGF, Kormelink R, Bai Y, Wolters A-MA. **2020**. The NLR Protein Encoded by the Resistance Gene Ty-2 Is Triggered by the Replication-Associated Protein Rep/C1 of Tomato Yellow Leaf Curl Virus. *Frontiers in Plant Science* **11**.

Sõmera M, Fargette D, Hébrard E, Sarmiento C, ICTV Report ConsortiumYR 2021. **2021**. ICTV Virus Taxonomy Profile: Solemoviridae 2021. *Journal of General Virology* **102**: 001707.

Suvi WT, Shimelis H, Laing M. **2021**. Farmers' perceptions, production constraints and variety preferences of rice in Tanzania. *Journal of Crop Improvement* **35**: 51–68.

Thiémélé D, Boisnard A, Ndjiondjop M-N, Chéron S, Séré Y, Aké S, Ghesquière A, Albar L. **2010**. Identification of a second major resistance gene to Rice yellow mottle virus, RYMV2, in the African cultivated rice species, O. glaberrima. *Theoretical and Applied Genetics* **121**: 169–179.

Traoré VSE, Néya BJ, Camara M, Gracen V, Offei SK, Traoré O. **2015**. Farmers'perception and impact of rice yellow mottle disease on rice yields in Burkina Faso. *Agricultural Sciences* **6**: 943–952.

Traoré O, Pinel-Galzi A, Issaka S, Poulicard N, Aribi J, Aké S, Ghesquière A, Séré Y, Konaté G,

Hébrard E, *et al.* 2010. The adaptation of Rice yellow mottle virus to the eIF(iso)4G-mediated rice resistance. *Virology* **408**: 103–108.

Traore O, Pinel-Galzi A, Sorho F, Sarra S, Rakotomalala M, Sangu E, Kanyeka Z, Sere Y, Konate G, Fargette D. **2009**. A reassessment of the epidemiology of Rice yellow mottle virus following recent advances in field and molecular studies. *Virus Research* **141**: 258–267.

Wang M, Yu Y, Haberer G, Marri PR, Fan C, Goicoechea JL, Zuccolo A, Song X, Kudrna D, Ammiraju JSS, *et al.* 2014. The genome sequence of African rice (Oryza glaberrima) and evidence for independent domestication. *Nature Genetics* **46**: 982–988.

Wang J, Chai J. **2020**. Structural Insights into the Plant Immune Receptors PRRs and NLRs. *Plant Physiology* **182**: 1566–1581.

Wei F, Wing RA, Wise RP. **2002**. Genome Dynamics and Evolution of the Mla (Powdery Mildew) Resistance Locus in Barley. *The Plant Cell* **14**: 1903–1917.

Wilm A, Aw PPK, Bertrand D, Yeo GHT, Ong SH, Wong CH, Khor CC, Petric R, Hibberd ML, Nagarajan N. **2012**. LoFreq: a sequence-quality aware, ultra-sensitive variant caller for uncovering cell-population heterogeneity from high-throughput sequencing datasets. *Nucleic acids research* **40**: 11189–201.

Wu J, Ding J, Du Y, Xu Y, Zhang X. **2007**. Genetic analysis and molecular mapping of two dominant complementary genes determining resistance to sugarcane mosaic virus in maize. *Euphytica* **156**: 355–364.

Xi Y, Chochois V, Kroj T, Cesari S. **2021**. A novel robust and high-throughput method to measure cell death in Nicotiana benthamiana leaves by fluorescence imaging. *Molecular Plant Pathology* **22**: 1688–1696.

Yang Z, Li Y. **2018**. Dissection of RNAi-based antiviral immunity in plants. *Current Opinion in Virology* **32**: 88–99.

Zhao F, Cai Z, Hu T, Yao H, Wang L, Dong N, Wang B, Ru Z, Zhai W. **2010**. Genetic analysis and molecular mapping of a novel gene conferring resistance to Rice stripe virus. *Plant Molecular Biology Reporter* **28**: 512–518.

Table 1 Coat protein (CP) polymorphisms in natural rice yellow mottle virus (RYMV) populations at the positions mutated in samples from infected Tog5307 plants.

Position[1]	Amino acid (number of isolates)[2]	Alternate amino acid in Tog5307 samples
36	P (595)	S, R
37	V (581), M (14)	M
39	Q (594), H (1)	R
41	S (595)	P
56	W (593), C (1), L (1)	S
93	A (594), G (1),	V
103	R (570), K (13), Q (12)	W
130	D (594), G(1)	N
163	G (595)	D
166	R (595)	Q
224	I (594), V (1)	N
230	R (595)	W

[1] Positions refer to the sequence of the CIa isolate

[2] The sequences of the coat protein of the set of 595 isolates described in Issaka *et al*. (2021) and available in public databases were used. Residues in grey correspond to the reference sequence from the CIa isolate.

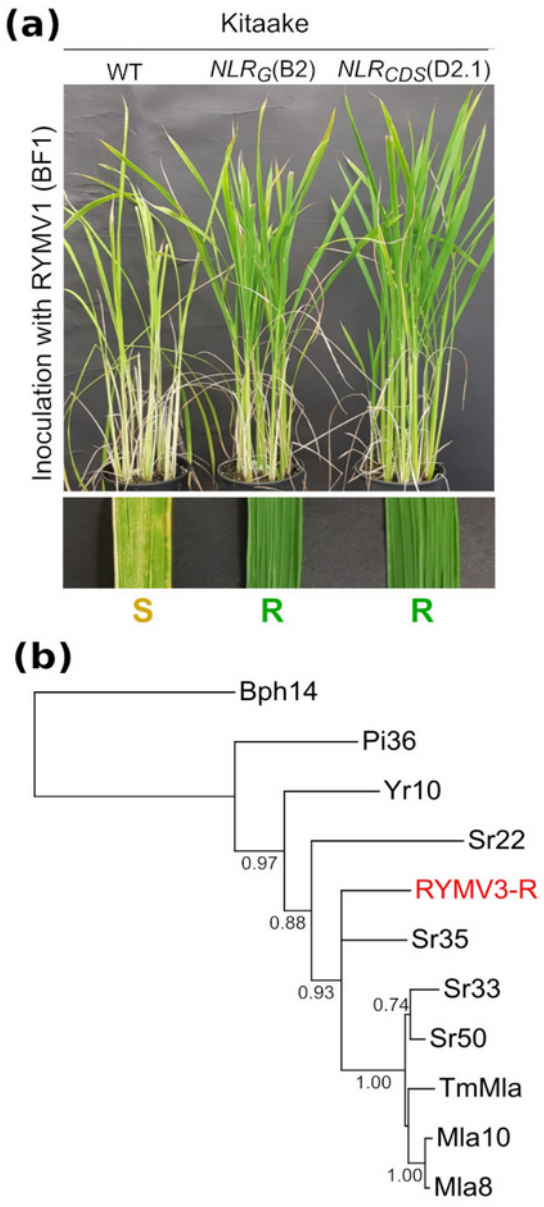

Fig. 1 *RYMV3* (*Resistance to rice yellow mottle virus 3*) encodes a nucleotide-binding and leucine-rich repeat domain protein (NLR) immune receptor related to Sr35 (Stripe rust 35) and to the Mla (Mildew locus A) family. (**a**) Kitaake wild-type (WT) and transgenic plants carrying the genomic construct NLR_G (T2 family B2) or the coding sequence (CDS) construct NLR_{CDS} (T3 family D2.1) were inoculated with the RYMV isolate BF1. Pictures were taken six weeks after inoculation. S: susceptible phenotype, R: resistant phenotype (**b**) Phylogenetic analysis of cereal NLR proteins closely related to RYMV3 based on the alignment of their NB-ARC domain (nucleotide-binding adaptor shared by APAF-1, certain *R* gene products and CED-4 – motif PFAM00931). Phylogenetic trees were inferred with PhyML+SMS using the JTT+G+I model. Branch supports were estimated with SH-like aLTR. The Bph14 resistance protein was used as an outgroup.

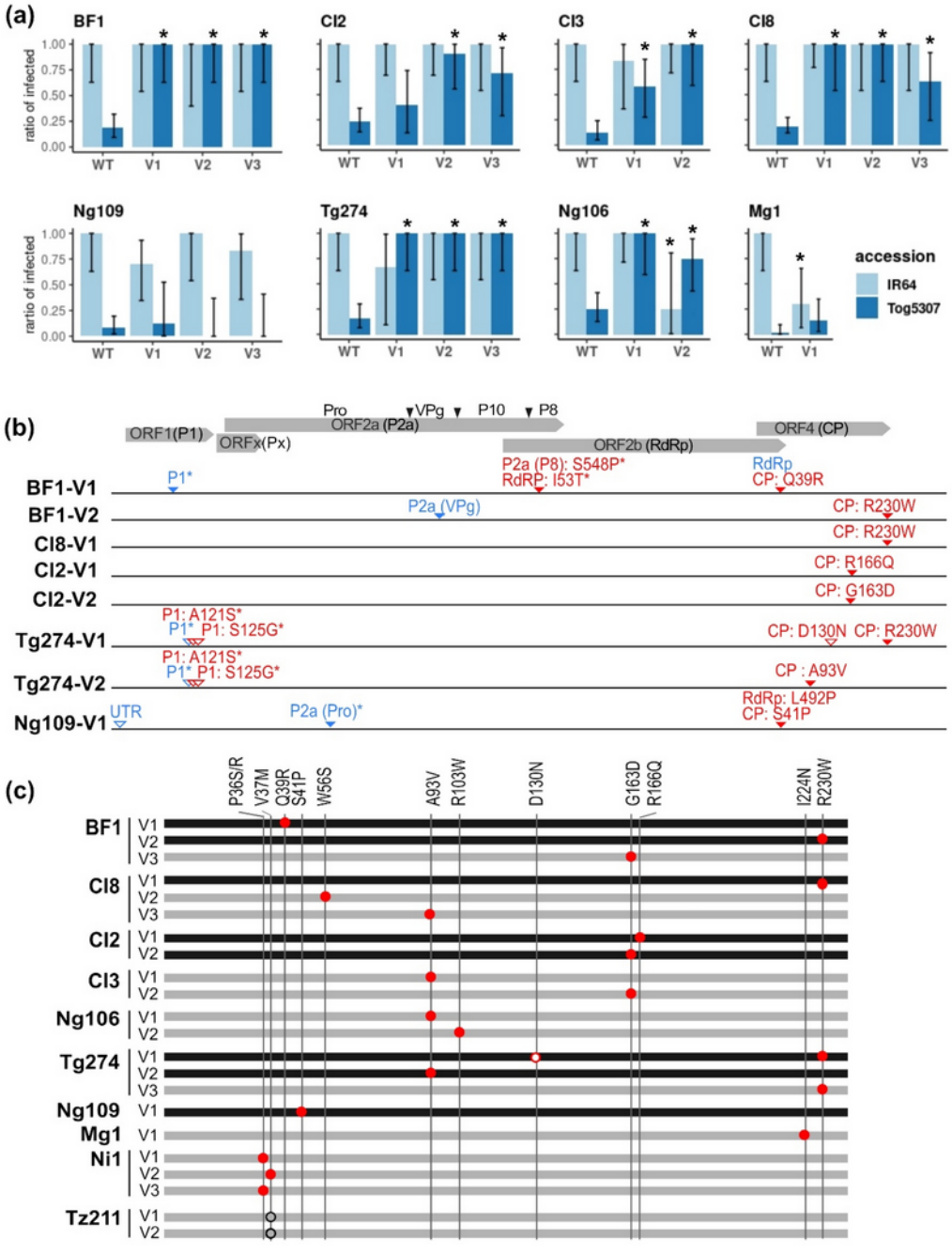

Fig. 2 RYMV3 (Resistance to rice yellow mottle virus 3) resistance breakdown is associated with mutations in the coat protein (CP). (**a**) Back-inoculation assays using extracts from RYMV-infected leafs of *Oryza glaberrima* Tog5307 (*RYMV3-R*) inoculated on Tog5307 and on the susceptible cultivar IR64. Infection rates caused by wild-type (WT) RYMV isolates (BF1, CI2, CI3, CI8, Ng109, Tg274, Ng106 and Mg1) were adopted from Pidon *et al*. (2017). Infection rates caused by spontaneous variants (V1, V2 and V3) were evaluated in this study. The error bars represent the 0.95 confidence intervals of the infection rates, based on the binomial distribution. Asterisks indicate significant differences to the infection rate obtained with the WT isolates determined by a Fisher exact test ($p<0.05$). (**b**) Mutations observed in the spontaneous variants used in (**a**) based on Illumina full-length genome sequencing. Synonymous single nucleotide polymorphisms (SNPs) or SNPs in non-coding regions are represented by blue triangles while non-synonymous SNPs are indicated by red triangles. Polymorphisms with a frequency of the alternate comprised between 0.1 and 0.5 are shown as open triangles and polymorphisms with a frequency of the alternate above 0.95 are indicated by filled triangle. Asterisks indicate mutations that were pre-existing in the corresponding WT isolate. The upper part of the panel shows the positions of the open reading frames (ORFs) and the putative cleavage sites of the P2a polyprotein. Some mutations affect two overlapping ORFs. (**c**) Mutations detected by Illumina or Sanger sequencing in the CP of RYMV samples from infected Tog5307 plants. Sequences obtained with Illumina and Sanger sequencing are represented as black and grey lines respectively. Filled red circles indicate mutations that were detected by Sanger or that were present in more than 95% of Illumina reads. The open red circle represents a mutation detected in Illumina with an alternate variant frequency of 0.1. The open black circles represent the M37 residue that is present in both the WT Tz211 isolate and V1 and V2 derived samples collected on Tog5307.

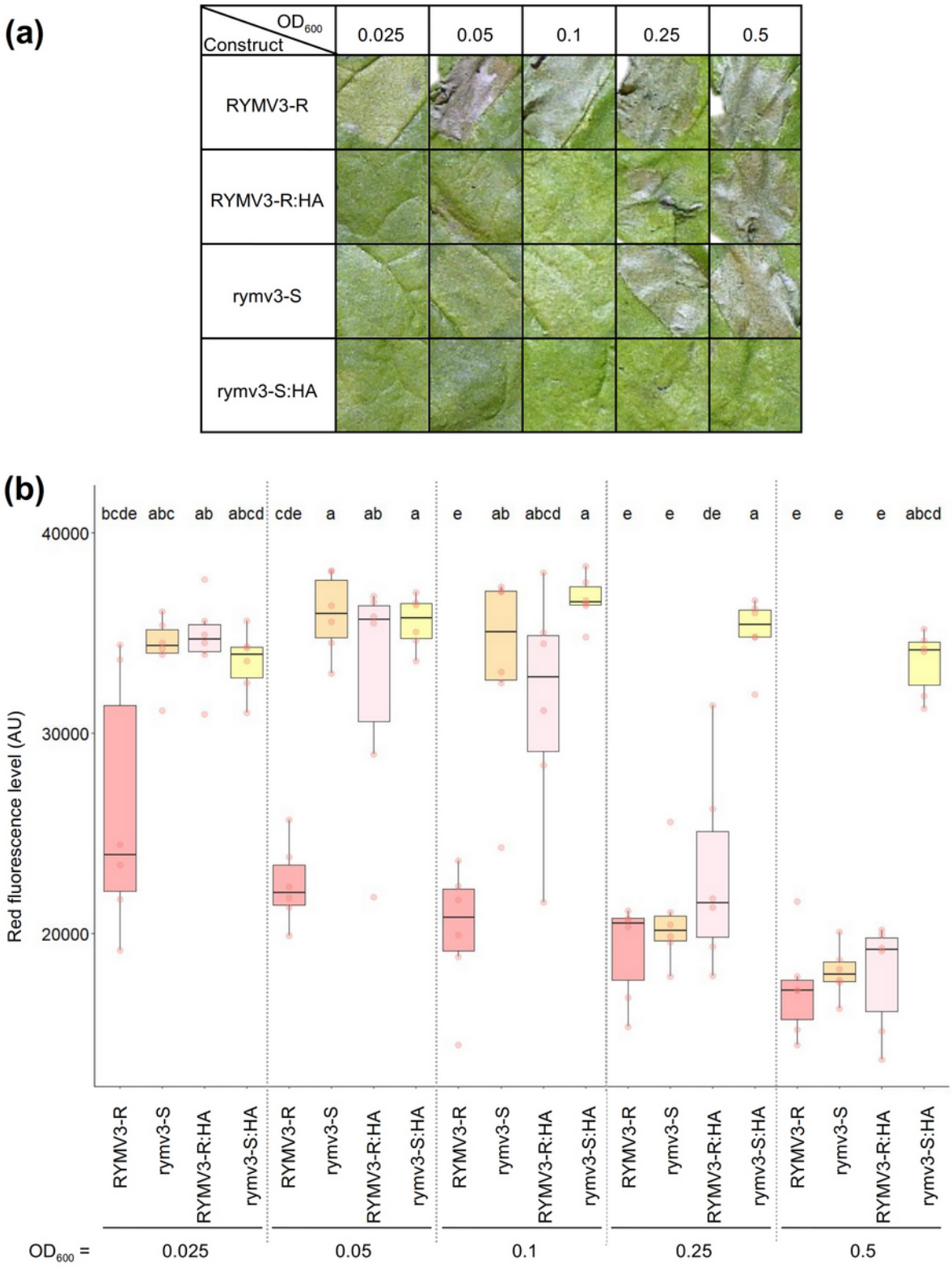

Fig. 3 RYMV3-R (Resistance to rice yellow mottle virus 3 – resistant allele) and rymv3-S (susceptible allele) are auto-active inducers of cell death. (**a**) The *RYMV3-R*, *rymv3-S*, *RYMV3-R:HA* and *rymv3-S:HA* constructs were transiently expressed in *Nicotiana benthamiana* leaves by *Agrobacterium tumefaciens* infiltration at inoculum density (OD_{600}) ranging from 0.025 to 0.5. Pictures were taken four days after agroinfiltration. (**b**) Cell death induced by the different combinations was quantified by measuring red fluorescence levels in *N. benthamiana* leaves four days after agroinfiltration. The boxes represent the first quartile, median, and third quartile. Lower and upper whiskers extend to respectively the lowest and highest value no further than 1.5 times the inter-quartile range (defined as the distance between the first and third quartiles). The pink dots indicate individual measurements from independent infiltration spots (n=6). Significant differences between conditions were estimated based on Kruskall-Wallis ($p<0.05$) and post-hoc Fisher tests (Bonferroni correction). Equivalent results were obtained in two independent experiments.

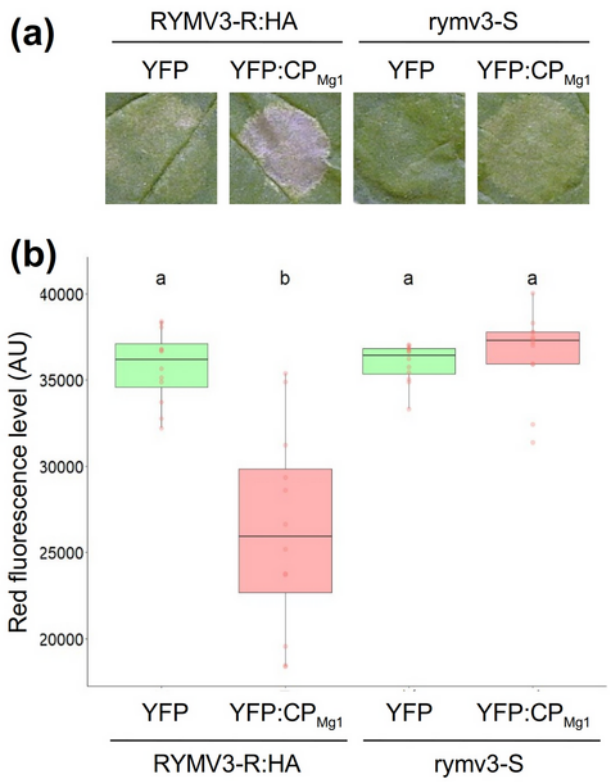

Fig. 4 RYMV3-R (Resistance to rice yellow mottle virus 3 – resistant allele) recognizes the coat protein (CP) of RYMV. (**a**) The *RYMV3-R:HA* and *rymv3-S* (susceptible allele) constructs were co-expressed with the yellow fluorescent protein (YFP) or YFP:CP_{Mg1} in *N. benthamiana* leaves by *A. tumefaciens* infiltration using inoculum densities (OD_{600}) of 0.05 for the *NLR* constructs and of 0.5 for the *YFP* and *YFP:*CP_{Mg1} constructs. Pictures were taken four days after agroinfiltration. (**b**) Cell death was quantified by measuring red fluorescence levels in *N. benthamiana* leaves four days after agroinfiltration. The boxes represent the first quartile, median, and third quartile. . Lower and upper whiskers extend to respectively the lowest and highest value no further than 1.5 times the inter-quartile range (i.e. the distance between the first and third quartiles). Red dots indicate individual measurements from independent infiltration spots (n=12). Significant differences between combinations were estimated based on Kruskall-Wallis ($p<0.05$) and post-hoc Fisher tests (Bonferroni correction). The experiment was preformed two times with equivalent results.

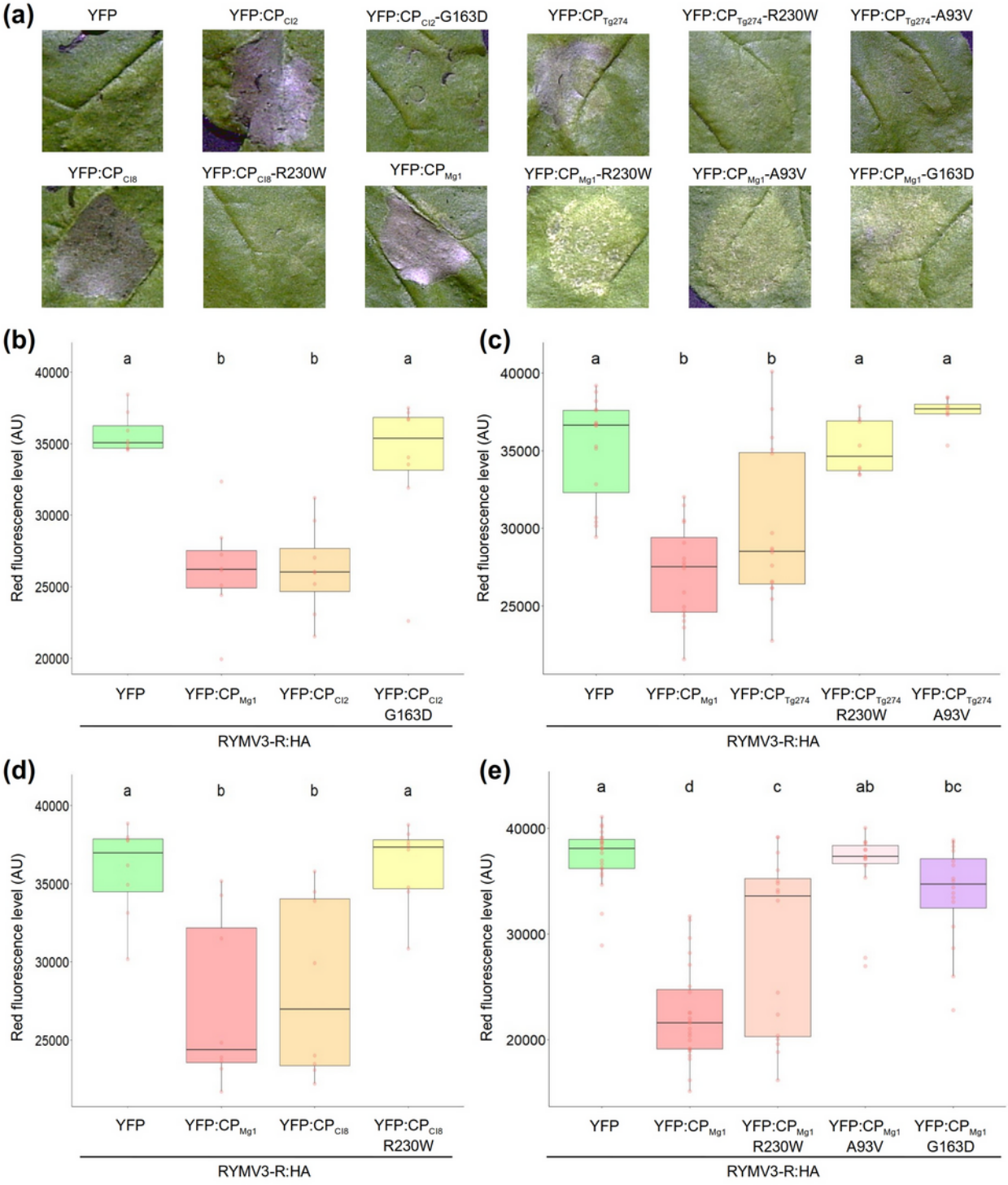

Fig. 5 Recognition of the coat protein (CP) is affected by resistance-breaking mutations. (**a**) The indicated *yellow fluorescent protein*:CP (*YFP:CP)* constructs from wild-type rice yellow mottle virus (RYMV) isolates (Mg1, CI2 , Tg274 and CI8) and corresponding mutants carrying point mutations (R230W, A93V and G163D) were transiently co-expressed with *RYMV3-R:HA* in *N. benthamiana* leaves. Inoculum densities (OD_{600}) of agrobacteria for the *YFP:CP* and the *RYMV3-R:HA* constructs were 0.5 and 0.05 respectively. Pictures were taken four days after agroinfiltration. (**b**), (**c**), (**d**) and (**e**) Cell death induced by the combinations of constructs agroinfiltrated in panel A was quantified by measuring red leaf fluorescence four days after agroinfiltration. The boxes represent the first quartile, median, and third quartile. Lower and upper whiskers extend to respectively the lowest and highest value no further than 1.5 times the inter-quartile range (i.e. the distance between the first and third quartiles). Red dots indicate individual measurements from independent infiltration spots (n=8 to 23). Significant differences between combinations were estimated based on Kruskall-Wallis ($p<0.05$) and post-hoc Fisher tests (Bonferroni correction). The experiments were performed twice with equivalent results.

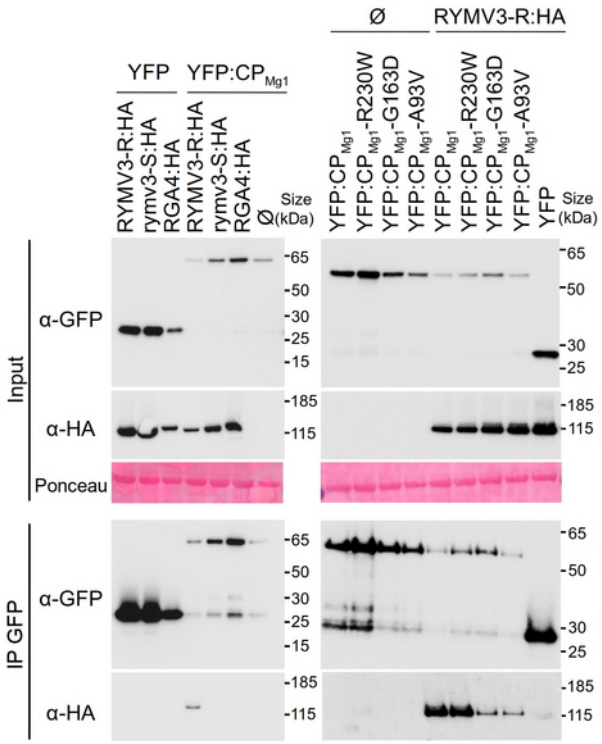

Fig. 6 Recognition of the coat protein (CP) involves formation of CP/RYMV3-R (Resistance to rice yellow mottle virus 3-resistant allele) complexes. Co immuno precipitation (Co-IP) experiments were performed using protein extracts from *N. benthamiana* leaves co-expressing the resistant or susceptible alleles of rice yellow mottle virus 3 protein, RYMV3-R or rymv3-S, C-terminally tagged with HA (OD_{600}=0.05) together with the Mg1 wild type or mutant CP fused to the yellow fluorescent protein (YFP) (OD_{600}=0.2). RGA4:HA (OD_{600}=0.1) and YFP alone (OD_{600}=0.2) were used as negative controls. Samples were harvested for total protein extraction 30 hours after agroinfiltration and analyzed by immunoblotting with anti-green fluorescent protein (α-GFP) and anti-HA (α-HA) antibodies (Input). Ponceau staining of the Rubisco small subunit was used to verify equal protein loading. Immunoprecipitations were performed with anti-GFP beads (IP GFP) and analyzed by immunoblotting with anti-GFP and anti-HA antibodies. Signals were detected with the Immobilon Western Kit (Millipore) on all blots with the exception of anti-HA probed IP samples in the CP mutant analysis (bottom right blot), where we used the more sensitive SuperSignal West Femto Maximum Sensitivity Substrate (Thermo Fisher Scientific).. The experiments were performed twice with equivalent results.

New Phytologist

***New Phytologist* Supporting Information**

Article title: Rapid evolution of an RNA virus to escape recognition by a rice NLR immune receptor

Authors: Mélia Bonnamy, Agnès Pinel-Galzi, Lucille Gorgues, Véronique Chalvon, Eugénie Hébrard, Sophie Chéron, Tràng Hiếu Nguyen, Nils Poulicard, François Sabot, Hélène Pidon, Antony Champion, Stella Césari, Thomas Kroj, Laurence Albar

Article acceptance date: 16 September 2022

The following Supporting Information is available for this article:

Fig. S1 Symptom expression on transgenic plants.

Fig. S2 Alignment of the NBARC domain of resistance proteins of the CNL family from grasses.

Fig. S3 Phylogenetic relationship of resistance proteins of the CNL family from grasses.

Fig. S4 Alignment of the NBARC domain of cereal NLR proteins closely related to RYMV3.

Fig. S5 Alignment of the NBARC domain of rice NLR homologous to RYMV3 and cereal NLR proteins closely related.

Fig. S6 Phylogeny of rice NLRs and cereal resistance proteins homologous to RYMV3.

Fig. S7 Immunoblot analysis of HA- and GFP- fusion proteins expressed in N. benthamiana.

Fig. S8 Comparison of the level of auto-activity of RYMV3-R:HA and rymv3-s.

Table S1 Sequences of primers.

Table S2 Description of constructs.

Table S3 Characteristics of RYMV isolates.

Table S4 List and characteristics of the CNL resistance proteins used for the phylogenetic analysis.

Table S5 Analysis of cosegregation between RYMV resistance and presence of the NLRG or NLRCDS construct in transgenic families.

Table S6 Similarity between NLR proteins closely related to RYMV3.

Table S7 Back-inoculation assays with infected Tog5307 leaves.

Table S8 Description of the Illumina sequencing datasets obtained from RYMV populations in infected Tog5307 or IR64 control leaves.

Table S9 Characteristics of the alternative variants identified in RYMV populations from infected Tog5307 or IR64 control leaves.

Table S10 Infection rates of isolates with a M37 residue in CP and control isolates with a V37 residue.

Table S11 Infection rates of mutant variants of the CIa infectious clone.

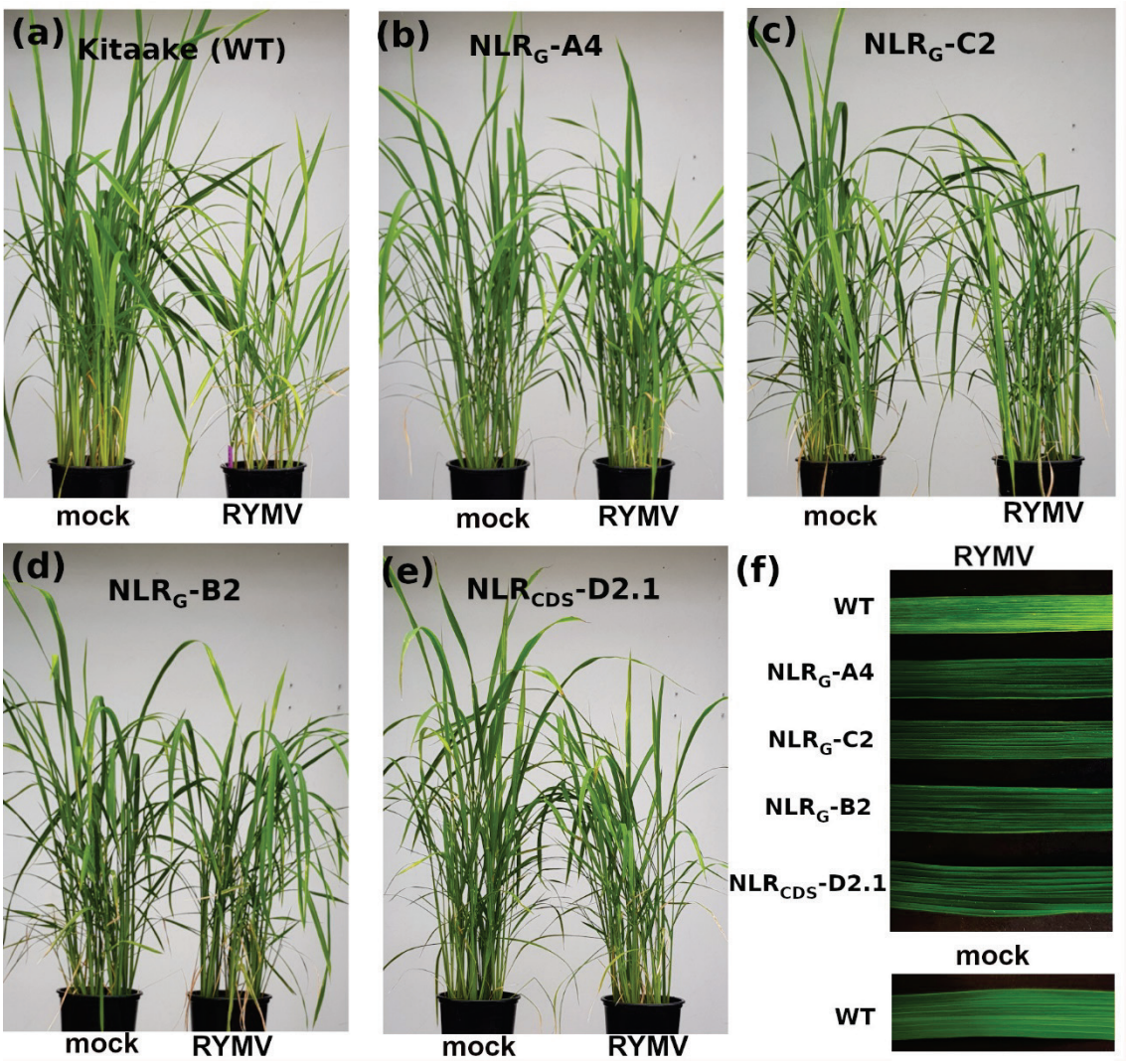

Fig. S1 Symptom expression on transgenic plants. Kitaake wild-type (WT) and transgenic T2 or T3 plants carrying the NLRG or NLRCDS constructs were inoculated with mock or with the RYMV isolate BF1. Plant development (a-e) and leave mottling and yellowing (F) were observed six weeks after inoculation. The T2 families NLRG-A2 (b), NLRG-C2 (c) and NLRG-B2 (d) derived from three different T0 plants were fixed for the NLRG construct; the T3 family NLRCDS-D2.1 was fixed for the NLRCDS construct (Table S5).

```
Mla6      1 -RLLSM--LKKVSIVGFGGLGKTTLARAVYEDFDCRAFVPKVLRDILNKRYLVIIDDIWDNLGSRLITTTRIVYQMEPLS
Mla2      1 -RLLSM--LKKVSIVGFGGLGKTTLARAVYEDFDCRAFVPKVLRDILNKRYLVIIDDIWDNLGSRLITTTRIVYQMEPLS
MLa13     1 -RLLSM--LKKVSIVGFGGLGKTTLARAVYEDFDCRAFVPKVLRDILNKRYLVIIDDIWDNLGSRLITTTRIVYQMEPLS
Mla12     1 -RLLSM--LKKVSIVGFGGLGKTTLARAVYEDFDCRAFVPKVLRDILNKRYLVIIDDIWDNLGSRLITTTRIVYQMEPLS
Mla10     1 -RLLSM--LKKVSIVGFGGLGKTTLARAVYEDFDCRAFVPKVLRDILNKRYLVIIDDIWDNLGSRLITTTRIVYQMEPLS
Lr1       1 EETVNRIFVSVLPIVGPGGIGKTTFAQHLYNHFQVRVWVCKLTREILSKRFLIVLDDIWKTKGSMLLVTTRFPLELLGLE
Lr10      1 HELVKWLRQKVVSIVGCAGLGKTTLAKQVYDNFEYRAFVSTILKCVLDKRYFVIIDDIWDSCGSVIMTTTRIVYNIQPLS
Bph14     1 QEIVSRLLLTVLPIVGMGGMGKTTLAQLIYNHFQLLLWVCLLAKSIVGQRYLLVLDDVWNGSGSSVLTTTRDPYDLKRLK
Mla8      1 -RLLSM--LKKVSIVGFGGLGKTTLARAVYEDFDCRAFVPKVLRDILNKRYLVIIDDIWDNLGSRLITTTRIVYQMEPLS
Pi2       1 KRLLEMIDAKVICVVGMGGLGKTALSRKIFENFPCNAWITELLKDMIEKRYFVVLDDLWIKKGSRIVITTRNVYHLDFLQ
Pita      1 QKLVRWLALKVASIVGSGGVGKTTLATEFYRPFDCRAFVRKILTDMLDKRYFIIIEDLWANSCSRILITTEIIIKIDPLG
Pi5-2     1 ENIKNLLLLPIIPIVGLAGLGKTAVAKLIFHNFDQRIWVHKIANSIIDQSSLIVLDDLFSKKGTKIIVTTSSPYKLGPLS
Pi37      1 -----------LAIVAHGGAGKSTLAQCVYNHFDVRMWVCRHTREIISEKFLLVLDDVWFQEGSRVLVTSRRVVHLENME
Pi36      1 --------TKIVYVVGMGGLGKTTLATAVYEGFPLNAFVPAILWNILGKRFFIVIDDIWDDYGSKILVTTRKVYNMKPLS
Pikp1     1 -----------VCILGLPGGGKTTVARELYDHFPCRVFVSKTLADIFNKKYLIVIDDIWHDLGGRIIMTTRLVYEVGDLD
Pikm      1 --------VKTICILGLPGGGKTTIARVLYHQFQCRVFASETLADIFNKKYLIVIDDIWHDLGGRIIMTTRLVYEVGDLD
Pid3      1 DLLMKWVKRMVVSVWGMGGIGKTALVANVYNDFDTCAWITDLLRRTANKRYVLVLDDVWNNIG-RIILTSRNIINLQPLE
Pia1      1 TKLNRWLSLKVAAIVGPAGIGKTALATELYRQFECRAFVRRLLGGILDRRYLIIIDGLWENSFSRILITADIIMRMEPLG
Pi9       1 KRLLEMIDAKVICVVGMGGLGKTALSRKIFENFPCIAWITELLKDMIEKRYFVILDDLWIKKGSRIVITTRNVYHLDFLQ
Rp1D      1 -----------LAIVGLGGMGKSTLAQYVYNCFDIRMWVCRHTREIISQKFLLVLDDVWFQSGSKVLVTSRSVIHLKNMD
Rdg2a     1 EVVVKLLLVQVLPIIGMGGLGKTTLAKMVYNHFELKMWHCALLKSIIQKRFMLVLDDVWNGPGSVILVTCRSPHELVFLN
Pm3a      1 KNIIGILVLTVVPVVAMGGLGKTTLAQLIYNHFQLLLWVCSLAKSIVGQRYLLVLDDVWDGMGSAVLTTTRDAYNLNALE
Pit       1 DMVKMIVSSTVFGIQGMGGIGKTTLAQKIYNKFQVHIWLCSLLKQAIGKSVFLVLDDVWKGLNSHILVTSRNTHKVNKMN
Sr22      1 DELVKWLNLKSVSIVGYGGLGKTTLANQIRVTFDCGAFVSAILRSILDTRYFIIIDDIWETLGSRIIITTRIVYEMKPLS
Rxo1      1 --------LRIIAVWGMGGVGKSTLVNNVYKNFDCRAWVSDIWKKMLKRQYLIILDDVWMGLGSRVIITTRIKIKVEPLG
TmMla     1 -----------VSIVGFGGLGKTTLARAVYEDFGCHAFVPKVFRDILNKRYRVIIDDIWDNLSSRLITTTRIIYQMKPLC
Sr50      1 -RLLSM--LKKVSIVGFGGLGKTTLARAVYDDFDCRAFVPKVLRDILNKRYLVIIDDIWDNLGSRLITTTRNIYKMKPLS
Sr45      1 --------LIVLPIVGMGGLGKTTFAQLVYNHFKLQRWCCKIANNICGKRYLIVLDDVWNGKGSAILTTTRNSHNLRNLD
Sr35      1 DKLINMLTLKTISIVGFGGLGKTTLAKAAYDQFDCGAFVSKVLKDILDKRYLIVIDDIWNSPGSRLITTTRNIYRMEPLS
Sr33      1 -----------VSIVGFGGLGKTTLAKAVYEDFDCHAFVPKVFRDILNKRYLVIIDDVWDNLGSRLIITTRIVYEIEPLS
Yr10      1 --------LKMVSIVGFGGLGKTTLANVVYEDFDCAAFVSKLFKCLLDKRYFILIDDIWDECGSRVIATTRIVYQLKPLS
Xa1       1 ETIKQLIMITVLPIVGNGGIGKTTLAQLVCKQFNVKIWVYKITRQILSKKFLIVLDDVWEATGNMIILTTRISIKLEALK
Pm2       1 EQIIGWLAIPIISVIGHGGMGKTALAQSICGHFKV-IWTTSVTSKILSINFLLVLDDVWETTGSKILLTTRMFLTLQGLE
RYMV3_R1  1 DELIGMLSLNIVSVVGFGGLGKTTLAKLVYDQFDCAAFVSKVLTDMINKRYIIIIDDIWDKLCSRIITTTRKIYRMKPLS
N         1 EKIESLLEVRIMGIWGMGGVGKTTIARAIFDQFDGACFLKSLQNALLSKKVLIVLDDIDNGNGSRIIITTRDIYEVTALP

Mla6     78 DILKKCGGVPLAIITIASALAILSFSYSNLPSHLKTCLLYLCVYPEDDKLIWKWVAEGFV-
Mla2     78 DILKKCGGVPLAIITIASALAILSFSYSNLPSHLKTCLLYLCVYPEDDKLIWKWVAEGFV-
MLa13    78 DILKKCGGVPLAIITIASALAILSFSYSNLPSNLKTCLLYLCVYPEDDKLIWKWVAEGFV-
Mla12    78 DILKKCGGVPLAIITIASALAILSFSYSNLPSNLKTCLLYLCVYPEDDKLIWKWVAEGFV-
Mla10    78 DILKKCGGVPLAIITIASALAILSFSYSNLPSNLKTCLLYLCVYPEDDKLIWKWVAEGFV-
Lr1      81 KIADKLKGSPLAAKTVGRLLHSLKISYDCLPFDLKKCFSYCGLFPEDSEINHFWVAVGIID
Lr10     81 DVLRKCGGLPLAINAISSLLAKLSLCYFDLPLHLRSCLLYLIMFPEDERLVHRWISEGFIR
Bph14    81 DIAKKCSGSPLAATALGSTLRILKLSYNCLPSYMRQCFSFCAIFPKDEMLIQLWMANGFIP
Mla8     78 DILKKCGGVPLAIITIASALAILSFSYSNLPSHLKTCLLYLCIYPEDDELIWKWVAEGFV-
Pi2      81 RIVNKCGRLPLAILTIGAVLAMVTLGYNHLPSHLKPCFLYLSIFPEDNRLVGRWIAEGFVR
Pita     81 DMIKKCGGLPLAITITARHFKVLNLIYNNLPHCLKACLLYLSIYKEDANLVRQWMAEGFIN
Pi5-2    81 QIVKRCEGIPAVAYSLGSLVRSFSEMYICMPSALKSCFAYLSTIPKGEKLIEQWIALDMVG
Pi37     70 KIAKRLGQSPLAARTVGSQLSALLWSYNKLDSRLQRCFLYCSLFPKGDEMVDLWVAEGLVD
Pi36     73 KILKKCAGVPLAIITIASLLAILPFSYYDLPSHLKNCLLYLSMFPEDNHLIWMWIAEGFV-
Pikp1    70 DIVNMCYGMPLALIWLSSALVSLCLGYNHLPLYLRTLLLYCSAYHWSGRLVRRWIAEGFVS
Pikm     73 DIVNMCYGMPLALIWLSSALVSLCLGYNHLPLYLRTLLLYCSAYHWSGRLVRRWIAEGFVS
Pid3     80 NFVDKCNGLPIAIVCIGRLLSILKISLEDLPHNIKNCFLYCSMFPENKSLVRLWVAEGFIE
Pia1     81 TILEKCGGLPLAIISIAGLLGTLNLSYNSLPHPFKTCLLYLGMYPDGADLMKQWSAEGFVS
Pi9      81 RIVNKCGRLPLAILTIGAVLAMVTLGYNHLPSHLKPCFLYLSIFPEDNRLVGRWIAEGFVR
Rp1D     70 EIAKRLGQCPLAAKVLGSRLCSLLWSYEKLDPRLQRCFLYCSLFPKGNELVHLWVAEGFVG
Rdg2a    81 RIVNKCGGLPLALKTMGGLLSILKLSYKHLSPEMKQCFAFCAVFPKDDRLIQLWMANGFIQ
Pm3a     81 EIVKRCCGSPLAATALGSVLCILKLSYNDLPSHMKQCFAFCAVFPKDAKLIQLWIANGFI-
Pit      81 QIVKKCDGLPLAIKVVAGVLSPLYLSYSNLPPELKQCFLWCALLPSNDAVAYWWVAEGFVT
Sr22     81 DILKKCRGLPLAINAISSVLVILSLSYFDLPHHLRSCLLYLALFPEDKRLVRRWISEGFI-
Rxo1     73 NIVEKCDGLPLALVAIGSILSIMNLSYKYLPDYLKNCFLYCAMFPEDKRLIRLWIAEGFIE
TmMla    70 DILKKCGGVPLAIITIASALAILSFSYYNLPPHLKTCLLYLCIYPEDDRLIWKWVAEGFV-
Sr50     78 DILKKCGGVPLAIITIASALAILSFSYYNLPSHLKTCLLYLCIYPEDDRLIWKWVAEGFV-
Sr45     73 KIMDRCGGSPLAAKAFGSMLSVLKLSYDDLPSHLKQCFAFCAVFPKDETLIQLWMAHDFI-
Sr35     81 EILKKCGGVPLAIITIASLLAILLFSYYDLPSYLKPCLLYLSIFPEDARLIWRWISEGFVY
Sr33     70 DILKKCGGVPLAIITIASALAILSFSYYNLPSHLKTCLLYLCIYPEDDRLIWKWVAEGFV-
Yr10     73 KILGKCGGVPLAIITLASMLAILHVSYYDLPPNLKTCLLYLSLYPEDKELIWKWIGEGFIH
Xa1      81 QIASELKGNPLAAKTVGSLLGALKLSYDHLSNPLQQCVSYCSLFPKGAQLIQIWIAQGFVE
Pm2      80 QIAKKLRGCPLVTKVVAEHLQVLRLSYYHLPTELQICFRYCCLFPQDKELVQMWIGSGLIA
RYMV3_R1 81 GILKKCAGMPLAIITIASLLAILSFSYYDLPCHLKTCLLYLSIFPEDDHLVRMWIAEGVVQ
N        81 EVVNYAKGLPLALKVWGSLLHKLKISYDGLEPKQQEMFLDIACF-----------------
```

Fig. S2 Alignment of the NBARC domain of resistance proteins of the CNL family from grasses.Alignment was performed with MAFFT v7.407_1 and then trimmed using BMGE v1.12_1 using NGPhylogeny web service (Lemoine et al, 2019).

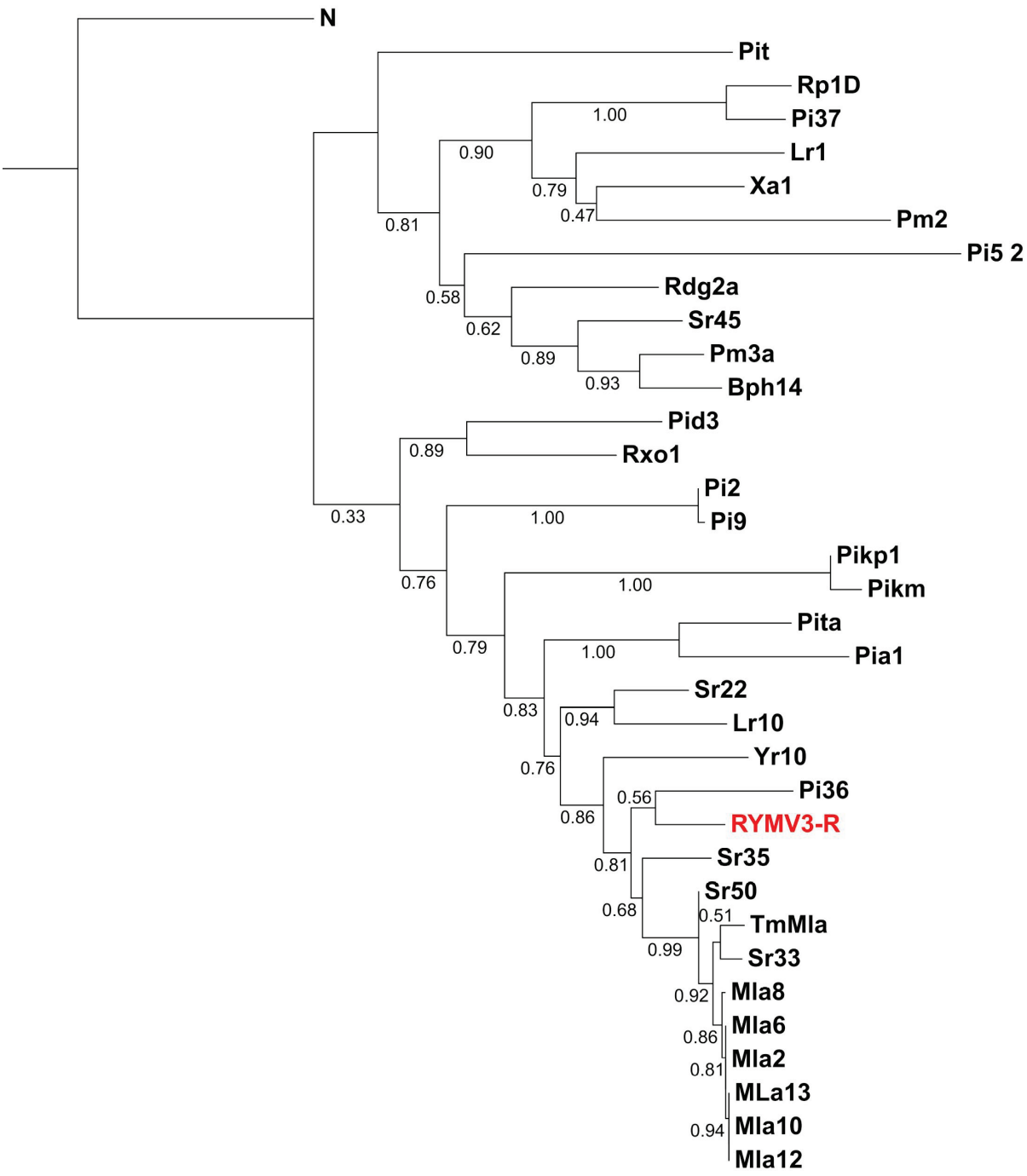

Fig. S3 Phylogenetic relationship of resistance proteins of the CNL family from grasses. Phylogenetic trees were based on the alignment of the NB-ARC domain and inferred with PhyML+SMS 1.8.1-1, and the LG+G model was selected. Branch supports were estimated with SH-like aLTR. The NB-ARC domain of the TNL N protein from N. tabacum was used as outgroup.

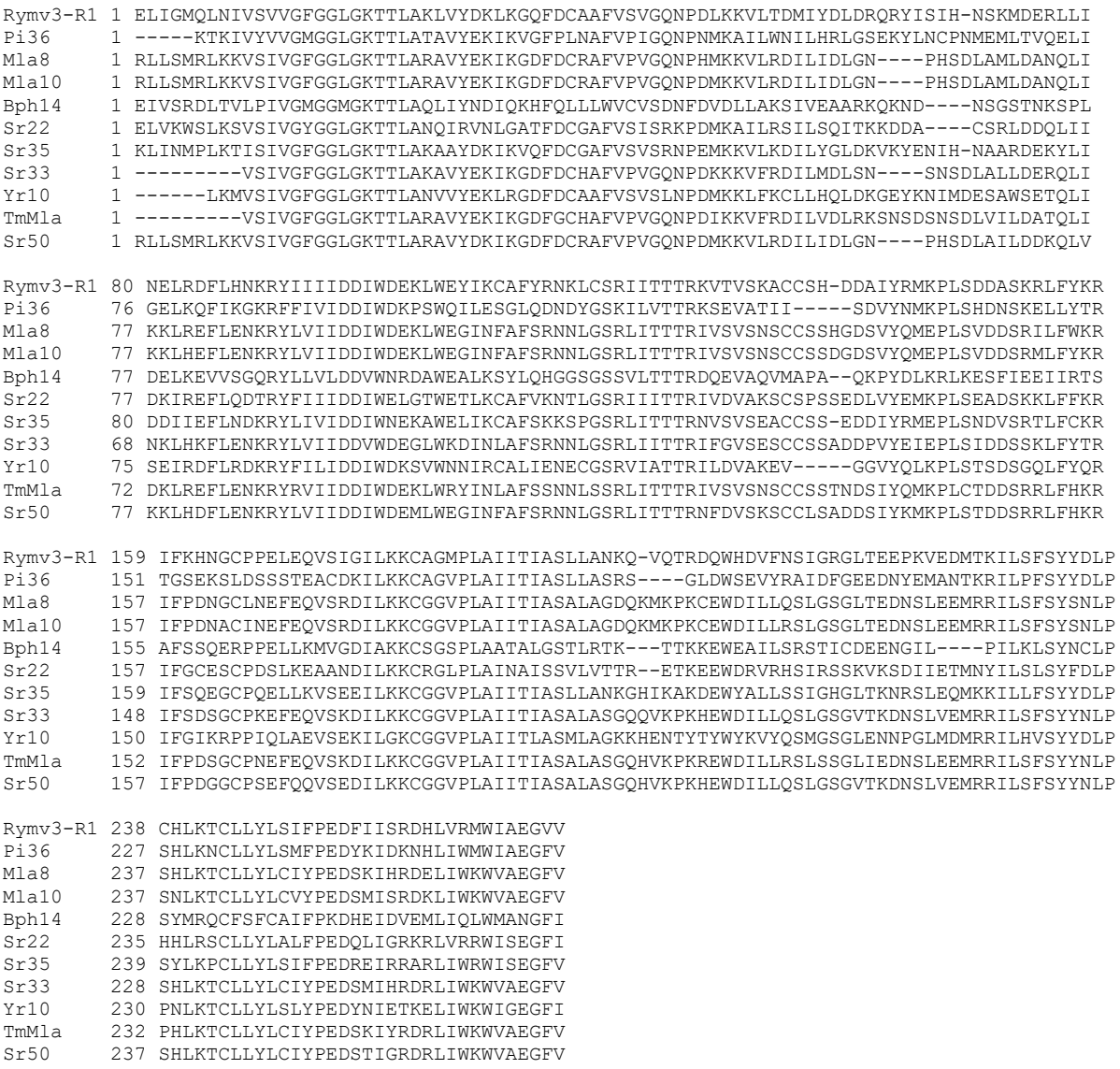

Fig. S4 Alignment of the NBARC domain of cereal NLR proteins closely related to RYMV3. Alignment was performed with MAFFT v7.407_1 and then trimmed using BMGE v1.12_1 using NGPhylogeny web service (Lemoine et al, 2019).

Lemoine F, Correia D, Lefort V, Doppelt-Azeroual O, Mareuil F, Cohen-Boulakia S, Gascuel O. **2019**.
NGPhylogeny.fr: new generation phylogenetic services for non-specialists. *Nucleic Acids Research* **47**: W260–W265

```
Os08g01580 1 TSLYQSLVGIDGPSQELIQLLQLKVVSVVGFGGLGKTTLAKYVYDKIGHQFDCTAFVSVSHKPDITRILSSIQSKLQLIDDIRAYLEHERYIIIVDDLWKIISCAFPNNGKG
Os07g27370 1 SALYTRLVGIDGPKDKIIKWLRLRTMAIVGCGGLGKTTLANQVYLEVKNQFDCSAFVTVSQNPDVKHVLAKFLSDVHLINKLREYLQDKRYFLVIDDIWDIIECALVKNSQG
Os06g33360 1 LLSNTKLVGIDGTRNDIIKILKMIKVSIVGSGGMGKTTLSRAVYDSVKGKFQCSAFVPVGQNQDLKRVFMDVLNDLLLMNEVYDFLENKRYIIVIDDIWKMIAKVLGDSSCG
Os03g46550 1 PALFAGLVGIEGPRSTLVSWLQLKVISIVGFGGLGKTTLAKEVNHAVGAHFQLKAFVSVSRNLNPKKLICDVLSQIQLIPILREHLADKRYLIIIDDIWRLVKSALHDNSCQ
Os02g19890 1 IGIYGKLIGISGPKEELTKLLKLKVISIVGVGGLGKTTLANVIYQQLRGQFECHAFVSVSLKPDLKKVLSSILRQFEIINKIRDEIKEKRYLIVIDDIWECIECALIENDRG
Os01g41890 1 TALYVKLVSVDKARDELSELLQLRTVSVFGFGGLGKTTLARAVYESIREQFDCAAFVSVSRNPNITKIFRKLLFELQLIDELRSFLQSRRYLIVIDDLWDFIKCVLYENNLS
Os08g07330 1 QALYKELIGVDGPMDKIINMLKKKIISIVGFGGLGKTTLAKAVYDKLKPDFDCGAFVPVGRNPDMKKVLRDILIDLQLINGIKDLVEKKRSIVIIDDIWDLIRCALQDSNCG
Os08g07380 1 LSMYKELVGIEGPMDELMKMLKPKMVSIFGFGGLGKTTLAKAVYDKLKPSFDSGAFIPVGQNPNIRKVFRDILMDLQLINKLQEFLQKKRCFVVIDDIWDLIRCALQDSNHE
Os08g07340 1 QALYKELIGVDGPMDKIINMLKKKIISIVGFGGLGKTTLAKAVYDKLKPDFDCGAFVSVGRNPDMEKVLRDILIDLQLINEIKDLVEKKRCFIVVDDIWDLIKCALQDSNCG
Os08g28600 1 GALFTHLVGIDGPRDDLVSWLHRKVLSIYGFGGLGKTTLANEVRRKIGPQFGCAALVSVSQKPDFKKILWGILSRIMLIEKIREILQDKRYFIIIDDIWSVLKCALPENKNG
Os08g28570 1 ----------QPKVISIVGFGGLGKTTLAYQVYQELKGKFDCSAFLSVSRNPNMMRILRTILSEVQLIIKISNFLSNKRYLIVIDDIWKIIKGAFSMSSQC
Os08g28540 1 LSIFENLVGIEGPKNEVIKLLHPKVVSVVGFGGLGKTTLAYQVYQQLKGNFSCSVFVSVSRNPDMMRILRTILSEVQLIIKISNFLSKKRYFVVIDDIWNIIKGAFSMNSRC
Os08g10440 1 TALYQNLVGIDGPTEELIQLLKLMVVSIVGFGGLGKTTLAKQVYDKIGQQFDCKAFVSVSQRPDIARLLRTIQSKFDIIDDIRYYLGNKRYLIVVDDLWKIIHCAFPENSNG
Os08g10430 1 ----------MVVSIVGFGGLGKTTLAKQVYDKIGQQFDCKAFVSVSQRPDIARLLSTIQSKLDIIDGIRYYLGNKRYLIVVDDLWKIISCAFPENANG
Os08g10260 1 ----------PREQVIKWLQIMVLPIVGFGGLGKTTLAKEVYQKIGQQFNTTEFVSVSQRPDVTRFLKGIQSKLDIIDNIRAYLQHRRYLFVVDDLWDIIRSVFPENGMG
Os08g31800 1 PALFERLVGIEGPRDELVEFLQRRVVSIVGFGGLGKTTLANQVYQHIKSQFDRTAFVSVSRNPNVNKILANILIGIKLISLIRENLQNSRYFIVIDDIWDHLRFAFPENNSA
Os08g29854 1 TALYVHLVGLDGPKLELIKMLKLVVVSIVGLGGLGKTTLANQVYHHLKPEFDCSAFVSVGQNPDVLKILDNILSGLVLVEKTRRFIADKRYLVLLDDIWNILRCSLPNNHLG
Os11g17330 1 PALYVNLVGIDTPRVELIRFLKLQVVSIVGIGGLGKTTLARQVYGKISGQFDCQAFVSVSQKPDIRKIFKNILINIRLINKLREFLNDKRYFVVIDDIWSTIRCAFCENYRG
Os11g16470 1 PAFYSGLVGIDGPRDKIIKLLRLKMVSIAGFGGLGKTTLAKQVYEKIKWQFDCAAFVFVSQIPDMKRVLLDLLCGLQLIDKIREFLHDKRYIIVIDDIWSILKCVLPENNSG
Os11g15500 1 PALYASLVGIDEPTNDIIKWLKLKVVSIWGPGGLGKTTLARQVYDKIGRQFDCQAFVSVSQKPDMRKVFRNILISVRLINKLRDFINCKRYFIVIDDIWSTIRCVLLDSNIG
Os11g15190 1 PALFAALVGIDEPAEELINWLRLSVVSVVGLGGLGKTTLARQVYNKIGGQFDCQAFVSISQKPDMRKIFQKMLNDIQLINKLRETLTGRRYFIVIDDLWSTIRCAFP-----
Os11g14380 1 SALYVRLVGIDAPRDEIIGRLQVMTISIVGCGGLGKTTLANQIYCKIKGKFECAAFASVFQNPNTKKVLTNILSQVAIINKLREYLSDKRYIVIVDDIWDFIECALVKNCRG
Os10g03570 1 TALYIDLVGIDHAREELIKTLQLKIISIVGFGGPGKTTLARAVHEKIEAQFDCSAFVSVSRNPDVRMIFKKMLHQLQLIDELREFLQDKRYFIIIDDLWDYIKCAFPKDNLG
Os11g37850 1 LTLYEKLVGIDKASNDLIKMLMLKMVSVVGFGGLGKTTLAKVVLDKLKVQFDCFGFIPVGQNPDIKKVLKDILIEVHMIDELREYLGNRRYLIVVDDIWEIIKCAFLDNNCG
Os11g37780 1 LALYENLIGVDKPADDLIKMLNLKMVSIVGFGGLGKTTLAKVVFDMLKGQFDCAGFVPVGQRPDIKRVFKDILIEVHLIDELREYLDNRRYLIIIDDIWEIIKCAFLDSNSG
Os11g37774 1 LTLYEKLVGIDKASDDLMRRLKLKMVSVVGIGGLGKTTLSKVVFDMLKLQFDCAAFVPVGQDHEIKKVLKDILVELHMINELREYLDNRRYLIVIDDIWEIIKLALIDSSCG
Os11g37759 1 LTLYEKLVGVDKASDDLMKRLKLKMVSVVGIGGLGKTTLSKVVFDKLKLQFDCAAFVPVGQNPEIKKVLKDILVELHMINELREYLDNRRYLIVIDDVWEIICALIDSNRG
Os11g37740 1 LTLYGKLVGIDKARDDLMKRLKLKMVSVVRIGGLGKTTLSKVVFDMLKLQFDCAAFVPVGQSPEIKKVLKDILVELHMINELREYVDNKRYLIVIDDVWDIIKCALIDSNCG
Os11g34920 1 SALYKELVGTKKKTDDLVSRLNLKVVSIVGFGGLGKTTLASVVYHKLKLEFDCGAFVSISLHPNMVGVFKNMLRQLQLIDELRKFLQNKRYIVVIDDIWSTIKYVLVDNQLG
Os11g32170 1 PALYTSLVGVDASVEEVIKLLKLKLVAIVGPGGIGKTTLANLVYQKLHGQFECQAFVSVSRKPNIKVVLSSILCQVEIIDKIRDILKDIRYFIIIDDIWDLLKCVLIDNDHG
Os11g37860 1 LGLYENLVGVDKASEDLIRMLMLKIVSVLGLGGLGKTTLAKFVFDNLKVQFQCFAFISVGQKPDIKNVLKHILIGLYLTDEVREYLDNKRYLIVIDDVWERINCALVDSNCG
Os11g43700 1 ----------EARDELIGMLQLNIVSVVGFGGLGKTTLAKVVYDKLRGQFDCAAFVSVGQNPDLKKVLTDMIYDLLLINELRDFVQNKRYIIIIDDIWDYIKCAFYRNKLC
Os12g37740 1 PAFYTRLVGIDGPRDKLIKMLQLKVVSIVGFGGLGKTTLANEVCRKLEGQFKYQAFVSVSQKPDIKKILRHILSQIQLIHTIRQFLKDKRYFIVIDDIWSTIKCAFPENNCS
Os12g17490 1 PALYVKLVGIHGPMEEIIELLKLKVVSIVGFGGLGKTTLANQVYNKIKDQFDCSAFISVSQSPNIKKILFDMLKDVQLIGKLRVFLENKRYFIIVDDIWSHVRLALPENSLC
Os12g17480 1 PALYVKLVRIDGPREKIIEWLKLKVVCIVGFGGLGKTTLANQVYHKMKGQFDCSSCMPVSRNPNMTKILVDLLKELQLICKLRTFLQRKRYLVIVDDIWSVVKCALPENNLC
Os12g17410 1 PVLYVKLVGIDGPREKIIEWLKLKVVCIVGFGGLGKTTLANQVYHKMKGQFDCSSFMPISRNPNITKILADLLKELQLICKLRTFLQCKRYLVIVDDIWSVVKCALPENNLC
Os12g17090 1 PALYERLVGIDGPREKIIKWIQRKVVSIVGLGGLGKTTLANEVYKTIQGDFKCITFVSISRTPNIRKILVDMLKGLNLISHLRGFLKDKRYLIVFDDIWDVVNCAFPENNLG
Os11g37880 1 LSLYENLVGIDKASNDIIKRLMLKMVSIVGFGGLGKTTLAKAVFDTLKVQFDCIGFVPVGQNPDIKKVLKDILIELHLIDELREYLDNKRYLIVIDDIWEIIKCALADSNCG
Os11g37870 1 LALYENLVGIDKTSDDLIKRLKLKLISIVGIGGLGKTTLAKAVFECLKMQFECAALIPVGQKPDIKKVFKDILIELYLIDELREYLHKRRYLIVIDDIWEMIKCALVDSNCG
Os12g37760 1 PSLYAGLVGIEQPRDVVIKLLKLKVISIVGPGGLGKTTLANEVFRKLESQFQCRAFVSLSQQPDVKKIVRNIYCQVKLINATREFLTNKRYFVVIDDIWSTIRCALFVNNCG
Os12g37770 1 PSLYAGLVGIETPRAVLVKLIQLKVISIVGPGGLGKTTLANEVYRRLEGQFQCRAFVSLSQQPDVKRILRNIFCQVNLIDAIRGFLKDKRYFIVIDDIWSTIKCALLMNNLG
RYMV3-R    1 ----------EARDELIGMLQLNIVSVVGFGGLGKTTLAKLVYDKLKGQFDCAAFVSVGQNPDLKKVLTDMIYDLLLINELRDFLHNKRYIIIIDDIWDYIKCAFYRNKLC
Yr10       1 ----------LKMVSIVGFGGLGKTTLANVVYEKLRGDFDCAAFVSVSLNPDMKKLFKCLLHQLQLISEIRDFLRDKRYFLIIDDIWDNIRCALIENECG
Sr50       1 ----------LRLKKVSIVGFGGLGKTTLARAVYDKIKGDFDCRAFVPVGQNPDMKKVLRDILIDLQLVKKLHDFLENKRYLVIIDDIWDGINFAFSRNNLG
Sr35       1 ---------IEETRDKLINMLPLKTISIVGFGGLGKTTLAKAAYDKIKVQFDCGAFVSVSRNPEMKKVLKDILYGLYLIDDIIEFLNDKRYLIVIDDIWNLIKCAFSKKSPG
Sr33       1 ----------VSIVGFGGLGKTTLAKAVYEKIKGDFDCHAFVPVGQNPDKKKVFRDILMDLQLINKLHKFLENKRYLVIIDDVWDDINLAFSRNNLG
Sr22       1 ---------IDGPKDELVKWLSLKSVSIVGYGGLGKTTLANQIRVNLGATFDCGAFVSISRKPDMKAILRSILSQILIIDKIREFLQDTRYFIIIDDIWETLKCAFVKNTLG
Pi36       1 ----------KTKIVYVVGMGGLGKTTLATAVYEKIKVGFPLNAFVPIGQNPNMKAILWNILHRLELIGELKQFIKGKRFFIVIDDIWDILESGLQDNDYG
Mla6       1 ----------LRLKKVSIVGFGGLGKTTLARAVYEKIKGDFDCRAFVPVGQNPDMKKVLRDILIDLQLIKKLHEFLENKRYLVIIDDIWDGINFAFSRNNLG
Bph14      1 ----------EDKQEIVSRLDLTVLPIVGMGGMGKTTLAQLIYNDIQKHFQLLLWVCVSDNFDVDLLAKSIVEAASPLDELKEVVSGQRYLLVLDDVWNALKSYLQHGGSG

Os08g01580 113 SRVIVTTRVQIYKIQPLNDSRKLFFDRVFRQYEEISEILKKCSGLPLAIVTVGSLLARDSLGASLEGMRNILNLSYKNLPLHLKTCLLYIGKYPEDYEIGRELVTEWIAEGIM
Os07g27370 113 SRIVTTTRIQVYEMKALCDSKRLFFRRIFNQLREAANILRKCGGLPLAIISISSLLAKSRINYDIETMAWVLSLSYFDLPHHLKTCLMYLSIFPEDYVIKKRLIGRWIAEGFI
Os06g33360 113 SRVIITTRIHVYEIKHLSDSRRLLHRRILSDLEEVCEILRKCEGVPLAIVTTSSLLEYRSIALHVDNTMKILSLSFYHLPYHLRTCLLYLSAFPEDYLIGKTLIWRWIGEGFV
Os03g46550 113 SRIITTTRIRIYYIEPLNESRELFFKRIFAHLEEVSEILKKCGGLPLAILSIASSLAKKSIGFTLEGMNKILLFSYYDLPTHLKACLLYLSIFPEDQVIESKLVWRWMSEGLI
Os02g19890 113 SRIITTSRVTVYKLQPLSNSKKLFYKRIFYELKDISKTLRKCEGVPLAIITIGSLLAHNLIGSHVENMRHILSISYYDLPAHLRACFLYLSIYPEDYNIQKQLIRRWISEGFI
Os01g41890 113 SRIITTTRKKIYEMKRLSDSKKLLYTRIFTELKQVSDILKKCDGVPLAIITIASLLALNSIGRGVDDMQKILSFSYYDLPPHLKTCLLYLSIFPEDYEIERRLIWRWIAEDFV
Os08g07330 113 SRVVVTTRICVYNMEPLSDSEKLLYTRIASPSAVACKILNKCDGVPLAIITIASLLAYNSIGFDVENTIKILSFSYYDLPSYLKACLLYLSIFQEDVEIDKLLIWKWIAEGFV
Os08g07380 113 SRVVTTTRIEVYKMHPLSESKKLLYTRIISTSVEACKILKKCGGVPLAIIIIASLLAYNSIGLDVDNTRRILSLSYYDLPLHLKPCLLYLSIFPEDYYIEKLLIWKWIAEGFV
Os08g07340 113 SIVVATTRIHVYKMEPLSDSKKLLYARLAGPPAVACKILNKCHSVPLAITTIASLLVYNSIGFDVENTRRILSFSYYDLPSHLKACLLYLSIFSEDVEIDKILIWKWIAEGFV
Os08g28600 113 SRVITTTRIRCYKIEPLSHSRMLLFKRVFGQITHVSDILRKCTGLPLAIVSIASLLASTSTGSDLEGMKTILSLSYNDLPHYLKPCLLYLSIFPEDYDIERSLVRRWIAEGLV
Os08g28570  92 SKIITTTRIHVYNIRPLNHSRHLFHRRLFNHLEEVSQILKKCDGLPLAIIAISGLLVKNSIGSSVDVMISILSLSYYDLPPHLKTCLLHLSIFPEDYLIEKDLILRWVAEGFI
Os08g28540 113 SKIITTTRIHLYNIRPLDHSRTLFHRRLFNHLEEVSQILKKCDGLPLAIIAISGLLAKNSIGCTVEGMISILSLSYFDLPPHLKTCLLYLSIFPEDYVIRKDLILRWIAEGFI
Os08g10440 113 SRVIVTTRVYIYKMKALDDSKKLFFNRVFGQYEKVSEILKKCGGLPLAIITIASLLARNSLGTSLEGMRQILNLSYKNLPLHLRTCLLYLGNYPEDYKIGRDVVRQWIAEGFV
Os08g10430  90 SRVIVTTRVYIHRMKPLNDSKRLFFKRVIRQYEEVSEILKKCGGLPLAIITIASLLARNSLGTSLEGMRQILNLSYKNLPLHLRTCLLYLAKYPEDSSIDRDVVRQWIAEGFV
Os08g10260 101 CRIIVTTRSFIYRMEPLSNSRWLFFNRIFGQFREISQILKKCSGLPLAIITIASLLARNSIGTTLEGMRQILHLSYK--------------------------------
Os08g31800 113 SRIITTTRIFVYAMKPLSNSEALFFRRIFSELEEVADILKKCDGLPLAIVSIASLLSLNSFGSELAVVKRILFLSYSDLPHHLKSCLLYLSIFPEDHTITRFLISRWIAEGFI
Os08g29854 113 SRIITTTRIHIYKMGPLSDSQRLFFRRIFGQLKRISDILKRCRGLPLATLTIASILAHNSIGL--ENMNRILSLSFHDLPNHLKTCLLYLSIFPEDYVIERQLVWRWIAEGFI
Os11g17330 113 SKILCTTRINIYEMKPLSYAEKLFIKRIFGYLKDIYDILRRCGGLPLAIISLASLLARNSVCSSVSNMQRILSLSYNDLPHYLKTCLLYLSTFPEDVLILWPLVRRWIAEGFV
Os11g16470 113 SRIITTTRISIYRIKPLSDSRRLFCRRIFHHLEELSAILRKCGGLPLAILHIASLLALNSIGSTLQGLKKILLLSFYDLPPQLKTCLLYLSIYPEDCMINSELIRKWIAEGFI
Os11g15500 113 SRVLATTQIKVFEMKHLTHAEKLFLKRIFGHLKEVSGILRKCGGLPLAIITMASLLVRDSI--IVNRMQKILSLSYADLPHHLKTCLLYLSTFPEDCIIERRLVRRWIAEGFI
Os11g15190 108 --------NVYELKPLSDANKLFMKRIFGQLKLVSGILRKCGGLPLAIISIASLLARNSIGSSVNDMQRILSLSYNDLPHYLKTCLLYLSIYPEDFVIRRQLILRWIAEGFI
Os11g14380 113 SRIITTTRIYIYEMKPLGDSKILFDKRIFDQLTEVSEILKKCGGLPLAIISISSLLAKVSLSSDIETMEWVLSLSYSDLPNHLKTCLLYLSIFPEGYEINRRLVSRWIAEGFI
Os10g03570 113 SRLIITTRNIIYKMKPLSDSKKLFYKRIFPELEEVSEILKKCGGVPLAIITIASLLAHNSIGRNVEDMQKILSFSYYDLPSHLKSCLLCLSVFPEDYEIRRRLIWRWIAEGFV
Os11g37850 113 SRVIATTRIDVYSMAPLSNSKKLFYSRISRQLVEETKLIKKCGGVPLSIITMASLLVYESIGFVVQNTRKILSFSYYDLPSHLKTCMLHLSIYPEDSLIEKGLIWKWVAEGFV
Os11g37780 113 SRVIATARIYVYIMKPLSNSKKLFYSRIFGQPAEVTKLIKKCGGVPLSIITMASLLVYESIGFVVHNTRKILSFSYYDLPLYLKTCMLHLSIYPEDHLIEKCLIWKWVAEGFI
Os11g37774 113 SRVITTTRIDVYMMEPLSNSKTLFYNRIFGQSVEATKILKRCGGIPLSIITIASLLVYDSISFAVQNMRKILSFSYYHLPSYLKTCMLYLSIYPEDHLIYKILIWKWIAEGFV
Os11g37759 113 SRVIITTRIGVYMMEPLSNSKKLFYNRIFGQSVEATKILHKCGGIPLSIIAIASLLVYDSIGFAVQNTRKILSFSYYHLPSYLKTCMLYLSIYPEDHLIKKTLIWKWVAEGFV
Os11g37740 113 SRVITTTRIGVYIMEPLSNSKKLFYSRIFGQSVEATKILKKCGGIPLSIITSSLLVYDSIGFAVQNTRKILSFSYYHLPTYLKTCMLYLSIYPEDHLIGMTLIWKWVAEGFI
Os11g34920 113 SRIITTTRAGAYKLEPLSDSIKLFNQIIFHHLSEVSKILKKCGGIPLAIITIASMLAYHSMGSDLRNMRRILSISYYDLPPHLKTCLLYLSSYPEDYLSTRTLIWKWVGEGFV
Os11g32170 113 SKIITTTRNTIQIQQPLSDSEKLLYHKVFHQLQGISKILKRCGGLPLAIITIASLFACSSFHTDVKDMRWIISLSYCDMPSPLKTCFMYLSIFPEDYIIDRDLIWRWIAEDFI
Os11g37860 113 SKVITTTRIDVYRMKPLSNSKRLFNNRIFGQSVEATKILKKCNGMPLSIVTMASLLVYDSIGFEVENMRKILSFSYYELPSYLKTCLLYLSIYPEDHRIMKPLIWKWIAEGFV
Os11g43700 102 SRIITTTRKAIYRMKPLSASKRLFYKRIFKELEQVSGILKKCAGMPLAIITIASLLAFNSIGRKVEDMTKILSFSYYDLPCHLKTCLLYLSIFPEDFIISRHLVRMWIAEGVV
Os12g37740 113 SRILTTTRINVYEIKPLGHSKSLFFKRTFGHLKEVSAILRKCGGLPLGIITVASLLAHNSIGSDMEEMKRILLLSYDDLPYHLKTCLLYLSIIPEDYEIKRRLIRRWIAEGFI
Os12g17490 113 SRIITTTRNSVYNIQPLNDSKKLFLKRLFHHLEEVSAIIKKCHGFPLAIICLASLLAHNSLSS--QGMSDILLLSYYDLPYHLKTCLLYLSVFPEDYKIDRELIWRWIAEGFI
Os12g17480 113 SRVISTTRNYIHNMQPLTDSQKLFFKRIFGYLEQVSGIISKCHGLPLAIISIASLLAHNSIGF--QGIRDILLLSYYDLPINLKTCLLYLSVFPEDYKIDRELIWRWIAEGFI
Os12g17410 113 SRIISTTRNYIHNMQPLNDSQKLFYKRIFGYLEQVSGIISKCHGLPLALISIASLLAYNSIGF--QGIRDILLLSYYDLPIHLKTCLRYLSVFPEDYEIDRELIWRWIAEGFI
Os12g17090 113 SIIITTTRNYLHSMQPLEDSQRLFYRRAFNHLEDISAIISKCRSLPLAIISIASLLSHNSIGV--VEVRKILMLSYYDLPYPLKNCLLYLSMYPEDYVIDRELIWRWIAEGFI
Os11g37880 113 SKVITTTRIDVYNMAPLSNSKKLFNNRIFGELVAATRILKKCGGVPLSIITIASLLVYDSIGFVVQNTRKILSFSYYDLPSYLKTCLLHLSIYPEDHRIEKSLIWKWIGEGFV
Os11g37870 113 SRVITTTRINIYLMEPLSNSKKLFYNRMFGQQAEATKILQKCGGVPLSIITIACLLVYNSIGFAVQNTRKILSYSYYELPSHLKTCLLHLSIFPEDCWIEKSLIWIWIAEGFV
Os12g37760 113 SRIMTTTRNRVFEIMPLSNSKSLFLKRIFGQLDEVCEILKKCGGSPLAIITIASLLARNSIGSDVEEMRRILSLSYDDLPQHLKTCLLYLSIFPEDYEIERRLVERWVAEGFI
Os12g37770 113 SRIITTTRSHVYEIMPLSNAMSLFLKRIFGQLEEISKILKKCSGSPLAIITIASLLTHNSIGSSVEEMQRILSLSYDDLPHHLKTCLLYLCIFPEDCEIERQLVKRWIAEGFI
RYMV3-R    102 SRIITTTRKAIYRMKPLSASKRLFYKRIFKELEQVSGILKKCAGMPLAIITIASLLAFNSIGRKVEDMTKILSFSYYDLPCHLKTCLLYLSIFPEDFIISRHLVRMWIAEGVV
Yr10        91 SRVIATTRIGVYQLKPLSDSGQLFYQRIFGQLAEVSKILGKCGGVPLAIITLASMLAYQSMGSGLMDMRRILHVSYYDLPPNLKTCLLYLSLYPEDYNIETELIWKWIGEGFI
```

```
Sr50         93 SRLITTTRNSIYKMKPLSDSRRLFHKRIFPEFQQVSDILKKCGGVPLAIITIASALALQSLGSSLVEMRRILSFSYYNLPSHLKTCLLYLCIYPEDSTIGRRLIWKWVAEGFV
Sr35        104 SRLITTTRNDIYRMEPLSVSRTLFCKRIFSELLKVSEILKKCGGVPLAIITIASLLALSSIGHSLEQMKKILLFSYYDLPSYLKPCLLYLSIFPEDREIRRRLIWRWISEGFV
Sr33         88 SRLIITTRIPVYEIEPLSDSSKLFYTRIFSEFEQVSDILKKCGGVPLAIITIASALALQSLGSSLVEMRRILSFSYYNLPSHLKTCLLYLCIYPEDSMIHRRLIWKWVAEGFV
Sr22        104 SRIIITTRILVYEMKPLSDSKKLFFKRIFGSLKEAADILKKCRGLPLAINAISSVLVRHSIRSIIETMNYILSLSYFDLPHHLRSCLLYLALFPEDQLIGRRLVRRWISEGFI
Pi36         92 SKILVTTRKDVYNMKPLSNSKELLYTRTGSSSTEACKILKKCAGVPLAIITIASLLAYRAIDFEMANTKRILPFSYYDLPSHLKNCLLYLSMFPEDYKIDKHLIWMWIAEGFV
Mla6         93 SRLITTTRISVYQMEPLSDSRMLFSKRIFPEFEQVSDILKKCGGVPLAIITIASALALRSLGSSLEEMRRILSFSYSNLPSHLKTCLLYLCVYPEDSMISRKLIWKWVAEGFV
Bph14       102 SSVLTTTRDKPYDLKRLKFIEEIIRTSAFSELLKMVDIAKKCSGSPLAATALGSTLRLSRSTI--NGILPILKLSYNCLPSYMRQCFSFCAIFPKDHEIDVMLIQLWMANGFI
```

Fig. S5 Alignment of the NBARC domain of rice NLR homologous to RYMV3 and cereal NLR proteins closely related. Alignment was performed with MAFFT v7.407_1 and then trimmed using BMGE v1.12_1 using NGPhylogeny web service (Lemoine et al, 2019).

Lemoine F, Correia D, Lefort V, Doppelt-Azeroual O, Mareuil F, Cohen-Boulakia S, Gascuel O. **2019**.
NGPhylogeny.fr: new generation phylogenetic services for non-specialists. *Nucleic Acids Research* **47**: W260–W265

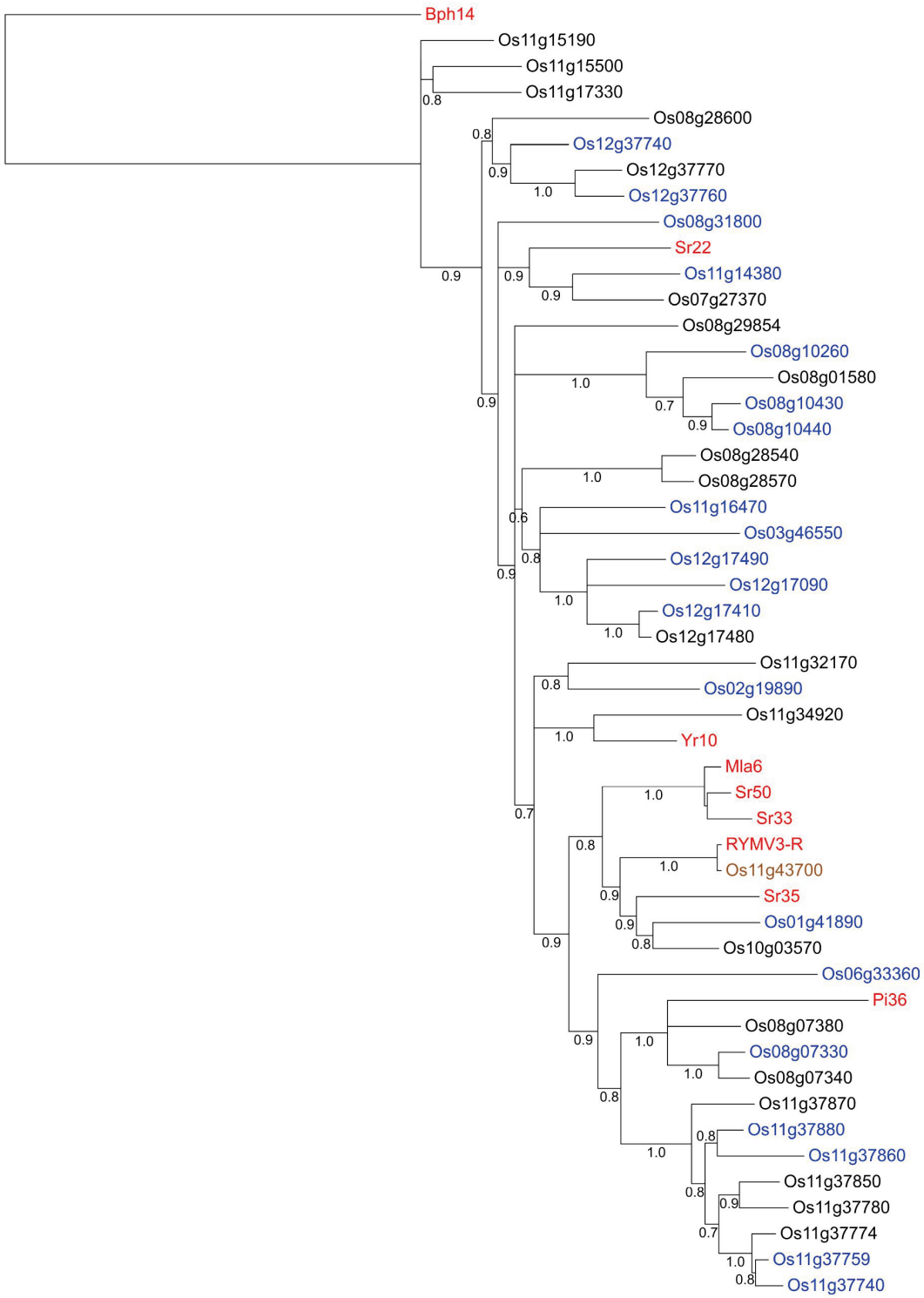

Fig. S6 Phylogeny of rice NLR homologous to RYMV3. Phylogenetic trees were based on the alignment of NLR's NB-ARC domain and inferred with PhyML+SMS 1.8.1-1, selecting the JTT+G+I+F model. Branch supports were estimated with SH-like aLTR. NLRs identified as resistance proteins in rice or other cereals are highlighted in red. The RYMV3 ortholog in Nipponbare is highlighted in brown. NLR genes with evidence of expression are indicated in blue.

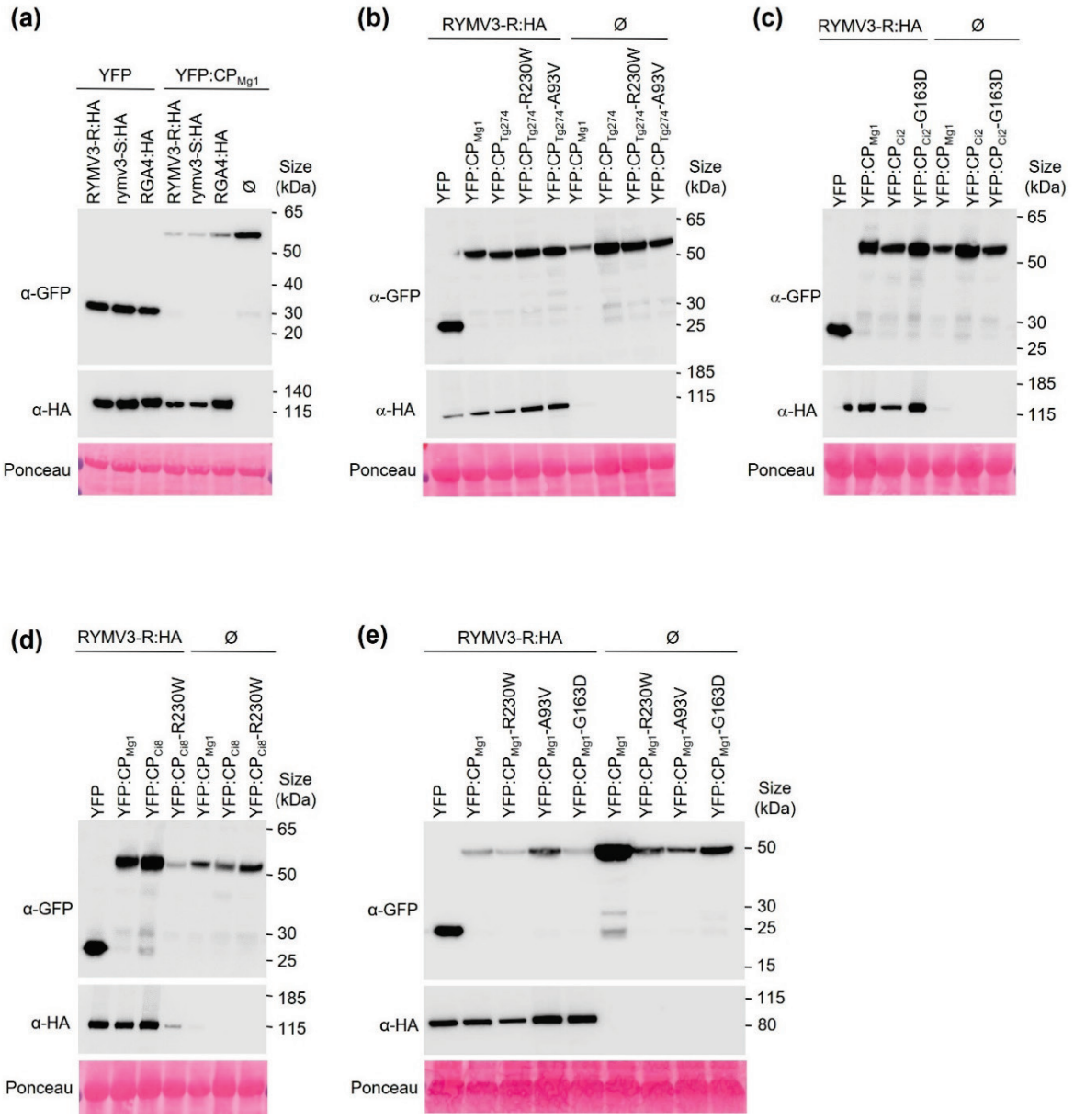

Fig. S7 Immunoblot analysis of HA- and GFP- fusion proteins expressed in *N. benthamiana*. HA-fusions of the NLRs Rymv3-R, rymv3-S and RGA4 were co-expressed with wild-type or mutant CPs of the RYMV isolates Mg1 (a-e), Tg274 (b), Cl2 (c) and Cl8 (d) in *N. benthamiana* leaves by infiltration of appropriate *A. tumefaciens* clones (OD_{600}=0.05 for RYMV3 constructs, OD600=0.1 for RGA4 and OD_{600}=0.2 for all CP constructs). Samples were harvested for protein extractions 30 hours after infiltration and analyzed by immunoblotting with anti-GFP (α-GFP) and anti-HA (α-HA) antibodies. Ponceau staining of Rubisco small subunit was used to verify equal protein loading.

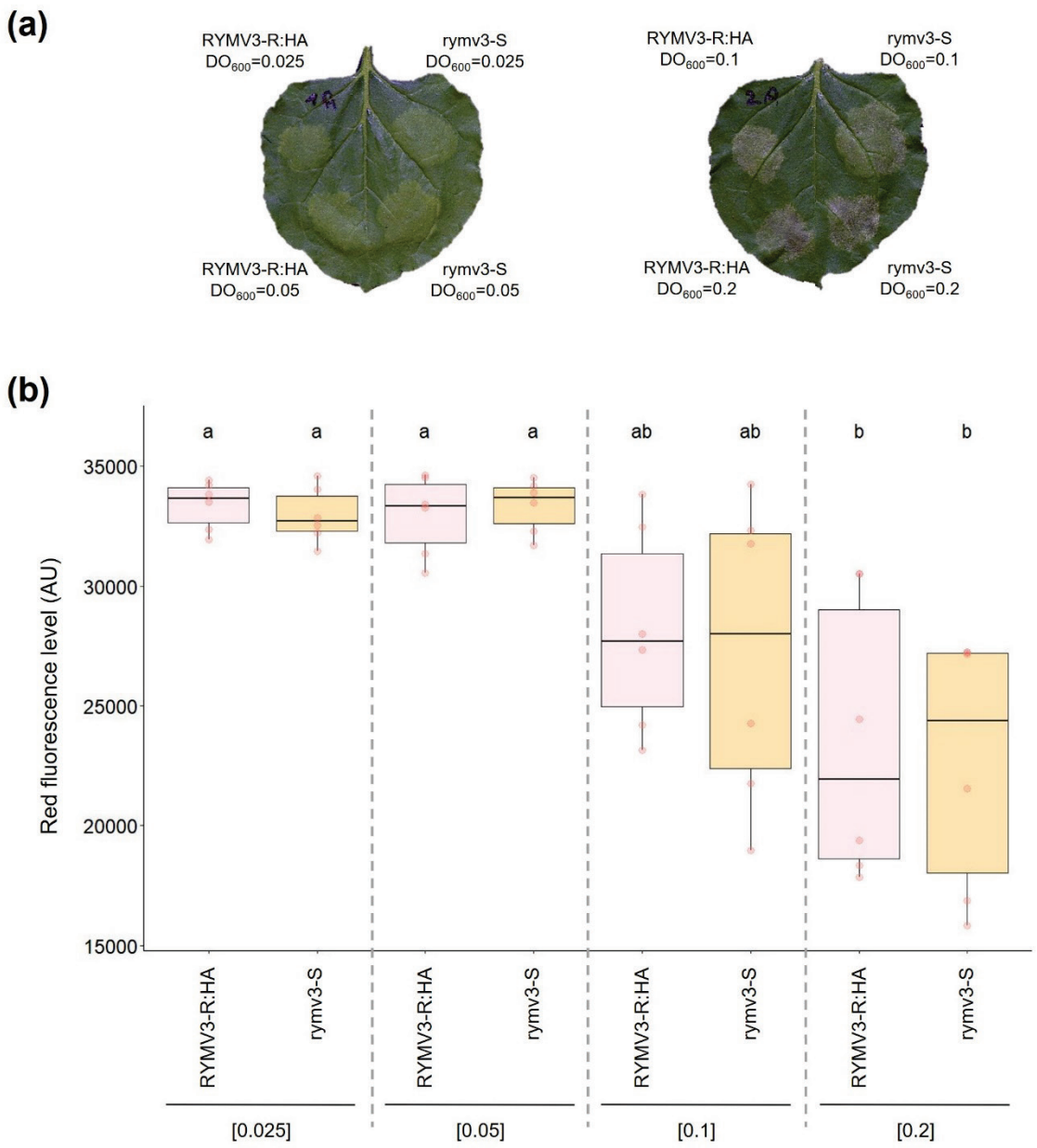

Fig. S8 Comparison of the level of auto-activity of RYMV3-R:HA and rymv3-s. RYMV3-R:HA and rymv3-S were expressed in *N. benthamiana* leaves by *A. tumefaciens* infiltration at bacterial density ranging from 0.025 to 0.2, as indicated in brackets. Pictures were taken four days after infiltration (a). Cell death was quantified by measuring red leaf fluorescence (b). The boxes represent the first quartile, median, and third quartile. Lower and upper whiskers extend to respectively the lowest and highest value no further than 1.5 times the inter-quartile range, i.e. the distance between the first and third quartiles). The red dots represent the measurement (n=6). Significative differences between conditions were determined by Kruskall-Wallis ($p<0.05$) and post-hoc Fisher tests (Bonferroni correction).

Table S1 Sequences of primers.

Target	Primer name	Sequence
Construct preparation		
NLR (RYMV3)	att-NLR-F2	GGGGACAAGTTTGTACAAAAAAGCAGGCTTATTTCATCTAGCGTGCAGGCA
NLR (RYMV3)	att-NLR-R2	GGGGACCACTTTGTACAAGAAAGCTGGGTCGGCCTCACATCCATCCTGTC
NLR (RYMV3)	att-RYMV3-F	GGGGACAAGTTTGTACAAAAAAGCAGGCTTAATGGAGCTCGCCATGGGTGC
NLR (RYMV3)	att-RYMV3-R	GGGGACCACTTTGTACAAGAAAGCTGGGTCTCAAGAACTTTCACTGGCCATG
NLR (RYMV3)	att-RYMV3-R-stop	GGGGACCACTTTGTACAAGAAAGCTGGGTCAGAACTTTCACTGGCCATGCTG
RYMV	att-CP-F	GGGGACAAGTTTGTACAAAAAAGCAGGCTTAATGGCCAGGAAGGGCAAG
RYMV	att-CP-R	GGGGACCACTTTGTACAAGAAAGCTGGGTCTCACGTATTGAGTGTTGGA
Screening of transformants		
Hygromycine resistance gene	HygR-F	CTCGGAGGGCGAAGAATCTC
Hygromycine resistance gene	HygR-R	GCTCCAGTCAATGACCGCTG
Ubiquitine promotor	Ubi	GGATGATGGCATATGCAGCAG
NLR (RYMV3)	NLR-R1	TCAGCTCATCTCTGGCCTCT
NLR (RYMV3)	NLR-S10R	AACATCTCGCAGGCACTCTC
NLR (RYMV3)	NLR-R8	ACATGCACATCTGCGCATTGTT
RYMV retro-transcription		
RYMV	RYMV-II	CTCCCCCACCCATCCCGAGAATT
Sanger sequencing of RYMV CP		
RYMV	RYMV-III	CAAAGATGGCCAGGAA
RYMV	RYMV-M	CGCTCAACATCCTTTTCAGGGTAG
Site-directed mutagenesis		
pENTRY-RYMV3-R	rymv3-s-F	CACATTCATGTACTTGGGATAAAaCCCATGTATTTCTTCACTGTA
pENTRY-RYMV3-R	rymv3-s-R	TACAGTGAAGAAATACATGGGtTTTATCCCAAGTACATGAATGTG
CIa isolate CP	CP-CIa-G163D-F	CACTTACTGAGTGGCGaCTCAGCACGAAATGCC
CIa isolate CP	CP-CIa-G163D-R	GGCATTTCGTGCTGAGtCGCCACTCAGTAAGTG
CIa isolate CP	CP-CIa-R230W-F	GTCAGTATGGTCCTGtGGGATCCGGTTGATC
CIa isolate CP	CP-CIa-R230W-R	GATCAACCGGATCCCaCAGGACCATACTGAC
CIa isolate CP	CP-CIa-V37M-F	CAACGGGCTCCG**a**TGGCTCAGGCCTC
CIa isolate CP	CP-CIa-V37M-R	GAGGCCTGAGCCA**t**CGGAGCCCGTTG
Mg1 isolate CP	CP-Mg1-R230W-F	ATGCTATCGTCAGTATGGTCCTGtGGGATCCGGTTGATCCAACACTC
Mg1 isolate CP	CP-Mg1-R230W-R	GAGTGTTGGATCAACCGGATCCCaCAGGACCATACTGACGATAGCAT
Mg1 isolate CP	CP-Mg1-G163D-F	GGGCTGCCATTTGTTGAATGGCGaTTCAGCACGGAATGCCGTGGTCG
Mg1 isolate CP	CP-Mg1-G163D-R	CGACCACGGCATTCCGTGCTGAAtCGCCATTCAACAAATGGCAGCCC
Mg1 isolate CP	CP-Mg1-A93V-F	TCTGCCTCGGGTGTGGAGTCTTGtACGTTGTTACTCGCTGTGGAAGC
Mg1 isolate CP	CP-Mg1-A93V-R	GCTTCCACAGCGAGTAACAACGTaCAAGACTCCACACCCGAGGCAGA

Table S2 Description of constructs.

This Table is provided as a separate file.

Table S3 Characteristics of RYMV isolates.

Isolate	Country of origin	Strain	Residue at VPg position 49	Residue at CP position 37	Reference
BF1	Burkina Faso	S2	T	V	Pinel et al., 2000
CI2	Côte d'Ivoire	S1	T	V	Pinel et al, 2000
CI3	Côte d'Ivoire	S1	T	V	Pinel et al, 2000
CI8	Côte d'Ivoire	S2	T	V	Pinel et al, 2000
CIa	Côte d'Ivoire	S2	T	V	Brugidou et al, 1995
Ma10	Mali	S1	E	M	Fargette et al 2004
Mg1	Madagascar	S4	E	V	Pinel et al., 2000
Ng106	Niger	S1	T	V	Traoré et al., 2010
Tg274	Togo	S1	T	V	Pidon et al., 2017
Tz2	Tanzania	S5	E	M	Pinel et al., 2000
Tz3	Tanzania	S5	E	M	Pinel et al., 2000
Tz5	Tanzania	S4	E	V	Fargette et al 2004
Tz9	Tanzania	S5	E	M	Fargette et al., 2008
Tz211	Tanzania	S5	E	M	Fargette et al., 2008

Brugidou C, Holt C, Yassi M N, Zhang S, Beachy RN, Fauquet C. **1995**. Synthesis of an infectious full-length cDNA clone of rice yellow mottle virus and mutagenesis of the coat protein. *Virology* **206**: 108–115.

Fargette D, Pinel A, Abubakar Z, Traore O, Brugidou C, Fatogoma S, Hebrard E, Choisy M, Sere Y, Fauquet C, *et al.* 2004. Inferring the evolutionary history of Rice yellow mottle virus from genomic, phylogenetic, and phylogeographic studies. *Journal of Virology* **78**: 3252–3261.

Fargette D, Pinel A, Rakotomalala M, Sangu E, Traore O, Sereme D, Sorho F, Issaka S, Hebrard E, Sere Y, *et al.* 2008. Rice yellow mottle virus, an RNA plant virus, evolves as rapidly as most RNA animal viruses. *Journal of Virology* **82**: 3584–3589.

Pidon H, Ghesquière A, Chéron S, Issaka S, Hébrard E, Sabot F, Kolade O, Silué D, Albar L. **2017**. Fine mapping of RYMV3: a new resistance gene to Rice yellow mottle virus from Oryza glaberrima. *Theoretical and Applied Genetics* **130**: 807–818.

Pinel A, N'Guessan P P, Boussalem M, Fargette D. **2000**. Molecular variability of geographically distinct isolates of Rice yellow mottle virus in Africa. *Archives of Virology* **145**: 1621–1638.

Traoré O, Pinel-Galzi A, Issaka S, Poulicard N, Aribi J, Aké S, Ghesquière A, Séré Y, Konaté G, Hébrard E, *et al.* 2010. The adaptation of Rice yellow mottle virus to the eIF(iso)4G-mediated rice resistance. *Virology* **408**: 103–108.

Table S4 List and characteristics of the CNL resistance proteins used for the phylogenetic analysis.

Gene name	Plant species	Pathogen	Genebank reference	Position of NB-ARC domain
Bph14	*Oryza sativa*	*Nilaparvata lugens*	ADB07392	180-464
Lr1	*Triticum aestivum*	*Puccinia triticina*	ABS29034	224-395
Lr10	*Triticum aestivum*	*Puccinia triticina*	AAQ01784	169-456
Mla10	*Hordeum vulgare*	*Blumeria graminis*	AAQ55541	180-459
Mla12	*Hordeum vulgare*	*Blumeria graminis*	AAO43441	180-459
Mla13	*Hordeum vulgare*	*Blumeria graminis*	AAO16014	180-459
Mla2	*Hordeum vulgare*	*Blumeria graminis*	ACZ65484	180-459
Mla6	*Hordeum vulgare*	*Blumeria graminis*	CAC29241	180-459
Mla8	*Hordeum vulgare*	*Blumeria graminis*	ACZ65486	180-459
Pi2	*Oryza sativa*	*Magnaporthe oryzae*	ABC94599	170-462
Pi36	*Oryza sativa*	*Magnaporthe oryzae*	ADF29624	190-458
Pi37	*Oryza sativa*	*Magnaporthe oryzae*	ABI94578	216-478
Pi5-2	*Oryza sativa*	*Magnaporthe oryzae*	ACJ54698	163-451
Pi9	*Oryza sativa*	*Magnaporthe oryzae*	ABB88855	170-462
Pia1	*Oryza sativa*	*Magnaporthe oryzae*	BAK39931	178-466
Pid3	*Oryza sativa*	*Magnaporthe oryzae*	ACN79513	177-463
Pikm	*Oryza sativa*	*Magnaporthe oryzae*	BAG71909	283-570
Pikp1	*Oryza sativa*	*Magnaporthe oryzae*	ADV58352	286-569
Pit	*Oryza sativa*	*Magnaporthe oryzae*	BAH20862	168-449
Pita	*Oryza sativa*	*Magnaporthe oryzae*	AAK00132	211-502
Pm²	*Triticum aestivum*	*Blumeria graminis*	CZT14023	199-458
Pm3a	*Triticum aestivum*	*Blumeria graminis*	AAY21626	179-455
Rdg2a	*Hordeum vulgare*	*Pyrenophora graminea*	ADK47521	170-452
Rp1-D	*Zea mays*	*Puccinia sorghi*	AAD47197	215-479
N	*Nicotiana glutinosa*	*Tobacco mosaic virus*	AAA50763	191-444
Rxo1	*Zea mays*	*Xanthomonas oryzae*	AAX31149	199-466
Sr22	*Triticum aestivum*	*Puccinia graminis*	CUM44200	178-460
Sr33	*Aegilops tauschii*	*Puccinia graminis*	AGQ17384	197-458
Sr35	*Triticum monococcum*	*Puccinia graminis*	AGP75918	171-462
Sr45	*Triticum aestivum*	*Puccinia graminis*	CUM44213	194-447
Sr50	*Secale cereale*	*Puccinia graminis*	ALO61074	183-462
TmMla	*Triticum monococcum*	*Blumeria graminis*	ADX06722	197-466
Xa1	*Oryza sativa*	*Xanthomonas oryzae*	BAA25068	304-591
Yr10	*Triticum aestivum*	*Puccinia striiformis*	AAG42168	194-464

Table S5 Analysis of cosegregation between RYMV resistance and presence of the NLRG or NLRCDS construct in transgenic families.

Construct	Generation	Family	Segregation[1]	
			with transgene	without transgene
NLR_G	T1	NLR_G-A	Sympt : 18 R ELISA : 24 R	Sympt : 2 S ELISA : 2 S
		NLR_G-B	Sympt : 9 R ELISA : 28 R	Sympt : 6 S ELISA : 3S
		NLR_G-C	Sympt : 41 R ELISA : 14 R	Sympt : 5 S ELISA : 1S
	T2	NLR_G-A1	0	Sympt : 12 S
		NLR_G-A3	ELISA : 18 R	0
		NLR_G-A4	ELISA : 16 R	0
		NLR_G-A5	Sympt : 15 R	Sympt : 1 S
		NLR_G-A6	ELISA : 16 R, 1 S	0
		NLR_G-B2*	ELISA : 15 R	0
		NLR_G-B3*	ELISA : 17 R	0
		NLR_G-B6	ELISA : 14 R	ELISA : 2 S
		NLR_G-C2*	ELISA : 16 R	0
		NLR_G-C3	Sympt : 16 R	0
		NLR_G-C5*	Sympt : 15 R	Sympt : 1 S
NLR_{CDS}	T1	NLR_{CDS}-D	Sympt : 8 R	Sympt : 8 S
	T2	NLR_{CDS}-D1	0	Sympt : 12 S ELISA : 9 S
		NLR_{CDS}-D2	Sympt : 6 R ELISA : 4 R	Sympt : 5 S ELISA : 1 S
		NLR_{CDS}-D6	Sympt : 8 R ELISA : 7 R	Sympt : 2 S ELISA : 2 S
		NLR_{CDS}-D7	Sympt : 8 R ELISA : 9 R	Sympt : 3 S ELISA : 1 S
		NLR_{CDS}-D9	Sympt : 5 R ELISA : 8 R	Sympt : 7 S ELISA : 3 S
		NLR_{CDS}-D10	Sympt : 16 R	Sympt : 4 S
		NLR_{CDS}-D11	0	Sympt : 18 S
		NLR_{CDS}-D12	0	Sympt : 17 S
		NLR_{CDS}-D14	Sympt : 9 R ELISA : 11 R	Sympt : 3 S ELISA : 1 S
		NLR_{CDS}-D16	Sympt : 8 R ELISA : 9 R	Sympt : 4 S ELISA : 2 S
	T3	NLR_{CDS}-D2.1	Sympt : 18R	0
	Kitaake (WT)			Sympt : 18 S

[1] The presence of the transgene was assessed by PCR. The resistance phenotype was either only determined by the observation of symptoms ("Sympt."), or in addition confirmed by an ELISA assay ("ELISA").

Table S6 Similarity between NLR proteins closely related to RYMV3.

	TmMla	Sr50	Sr35	Sr33	Sr22	Pi36	Mla8	Mla10	Yr10	RYMV3-R
TmMla		0.83[1]	0.51	0.87	0.44	0.36	0.81	0.81	0.45	0.42
Sr50	0.76[2]		0.53	0.83	0.46	0.36	0.81	0.81	0.46	0.47
Sr35	0.54	0.6		0.52	0.45	0.37	0.51	0.52	0.47	0.51
Sr33	0.81	0.8	0.55		0.45	0.36	0.81	0.81	0.45	0.46
Sr22	0.45	0.47	0.5	0.45		0.31	0.44	0.44	0.43	0.42
Pi36	0.45	0.47	0.44	0.47	0.4		0.37	0.36	0.32	0.35
Mla8	0.78	0.87	0.6	0.78	0.47	0.47		0.91	0.45	0.46
Mla10	0.77	0.86	0.59	0.78	0.46	0.47	0.96		0.46	0.46
Yr10	0.53	0.5	0.49	0.54	0.44	0.48	0.5	0.5		0.42
RYMV3-R	0.56	0.57	0.6	0.56	0.48	0.44	0.57	0.56	0.5	

[1] The upper part of the table indicates similarity rates calculated on the complete protein sequences.

[2] The lower part of the table indicates similarity rates calculated on the NB-ARC domain.

Table S7 Back-inoculation assays with infected Tog5307 leaves.

Isolate	Reference infection rates with WT isolate [1]	Back-inoculation tests[2]		
		Sample	Infection rate on Tog5307	Infection rate on IR64
BF1	Tog5307 : 10/53 IR64 : 8/8	V1	8/8**	6/6
		V2	8/8**	4/4
		V3	8/8**	6/6
CI8	Tog5307 : 21/112 IR64 : 8/8	V1	6/6**	14/14
		V2	8/8**	6/6
		V3	5/8*	6/6
CI2	Tog5307 : 13/56 IR64 : 8/8	V1	4/10	10/10
		V2	9/10**	10/10
		V3	5/7*	6/6
CI3	Tog5307 : 7/56 IR64 : 8/8	V1	7/12**	5/6
		V2	7/7**	11/11
Ng106	Tog5307 : 10/40 IR64 : 8/8	V1	7/7**	11/11
		V2	9/12*	1/4*
Tg274	Tog5307 : 7/44 IR64 : 8/8	V1	8/8**	2/3
		V2	8/8**	6/6
		V3	8/8**	6/6
Ng109	Tog5307 : 4/49 IR64 : 8/8	V1	1/8	7/10
		V2	0/7	5/6
		V3	0/8	6/6
Mg1	Tog5307 : 1/56 IR64 : 8/8	V1	3/22	3/10*

[1] Reference infection rates of wild type isolates were adopted from Pidon *et al* (2017)

[2] Leaf samples obtained by Pidon et al. (2017) after inoculation of different RYMV isolates were used to inoculate resistant Tog5307 and susceptible IR64 plants. Infected plants were identified 3 weeks after inoculation based on symptom expression and ELISA tests. The ratio between the numbers of infected and inoculated plants was compared to the reference infection rate with the corresponding wild-type isolates using Fisher exact test. Significant differences in infection rates at $p<0,05$ or $p<0,0025$ are indicated by "*" and "**" respectively.

Table S8 Description of the Illumina sequencing datasets obtained from RYMV populations in infected Tog5307 or IR64 control leaves.

Sample name	Total reads	Percentage of reads kept after cleaning	Properly mapped reads	Percentage of reads properly mapped	Minimum sequencing depth	Average sequencing depth
BF1-WT	269 778	94.4	226330	88.9	461	4768
BF1-V1	463 176	89.9	365104	87.7	890	5510
BF1-V2	472 006	90.5	352484	82.5	915	5989
CI2-WT1	487 592	94.5	420622	91.3	619	4976
CI2-V1	394 624	89.3	311252	88.3	748	5380
CI2-V2	581 814	89.8	446832	85.6	964	6893
CI8-WT1	537 578	95.5	447888	87.3	659	6817
CI8-WT2	144 788	95.4	106386	77.0	437	1993
CI8-V1	133 618	94.2	114118	90.6	485	2368
Tg274-WT	411 222	94.2	355290	91.7	443	6379
Tg274-V1	119 430	93.8	97636	87.2	244	1758
Tg274-V2	348 524	93.4	296416	91.1	448	4700
Ng109-WT	61 770	97.4	54204	90.1	245	1236
Ng109-V1	63 454	97.5	54204	87.6	289	1294

Table S9 Characteristics of the alternative variants identified in RYMV populations from infected Tog5307 or IR64 control leaves.

This Table is provided as a separate file.

Table S10 Infection rates of isolates with a M37 residue in CP and control isolates with a V37 residue.

Isolat	Residue at CP position 37	Infection rate[1]	
		IR64	Tog5307
Cla	V	4/4	0/11
Tz5	V	4/4	0/11
Tz2	M	4/4	10/12
Tz3	M	4/4	9/11
Tz9	M	4/4	8/8
Tz211	M	4/4	8/8
Ma10	M	4/4	8/8

[1] Infection rate was determined by ELISA tests 18 days after inoculation

Table S11 Infection rates of mutant variants of the CIa infectious clone.

Variant	Step 1: Infection rate with in vitro transcript[1]	Step 2: Infection rate with step 1 derived-samples
CIa	IR64 : 9/10 Tog5307 : 0/10	
CIa*CP:G163D[2]	IR64 : 4/10 (4 sequenced) Tog5307 : 0/10	IR64 : 1/5 (1 sequenced) Tog5307 : 4/20 (2 sequenced)
		IR64 : 0/5 Tog5307 : 2/20 (2 sequenced)
CIa*CP:R230W[2]	IR64 : 4/10 (4 sequenced) Tog5307 : 0/10	IR64 : 0/5 Tog5307 : 0/20
		IR64 : 0/5 Tog5307 : 3/20
Cia*CP:V37M	IR64 : 4/4 (4 sequenced) Tog5307 : 10/10 (10 sequenced)	

[1] In a first step, IR64 and Tog5307 plants were inoculated with in vitro transcripts. Infection was determined by ELISA tests or symptom observation two weeks after inoculation. The sequencing of infected samples confirmed the presence of the mutation.

[2] For CIa*CP:163D and CIa*CP:230W variants, two infected IR64 samples from step 1 were used as inoculum for back-inoculation on both IR64 and Tog5307. The infection rate was estimated as previously.